Determining Force Dependence of Two-Dimensional Receptor-Ligand Binding Affinity by Centrifugation

James W. Piper,* Robert A. Swerlick,# and Cheng Zhu*
*George W. Woodruff School of Mechanical Engineering, Georgia Institute of Technology, and #Department of Dermatology, Emory University School of Medicine, Atlanta, Georgia 30322 USA

ABSTRACT Analyses of receptor-ligand interactions are important to the understanding of cellular adhesion. Traditional methods of measuring the three-dimensional (3D) dissociation constant (K_d) require at least one of the molecular species in solution and hence cannot be directly applied to the case of cell adhesion. We describe a novel method of measuring 2D binding characteristics of receptors and ligands that are attached to surfaces and whose bonds are subjected to forces. The method utilizes a common centrifugation assay to quantify adhesion. A model for the experiment has been formulated, solved exactly, and tested carefully. The model is stochastically based and couples the bond force to the binding affinity. The method was applied to examine tumor cell adherence to recombinant E-selectin. Satisfactory agreement was found between predictions and data. The estimated zero-force 2D K_d for E-selectin/carbohydrate ligand binding was $\sim 5 \times 10^3$ μm^{-2}, and the bond interaction range was subangstrom. Our results also suggest that the number of bonds mediating adhesion was small (<5).

GLOSSARY

A_c	contact area (μm^2)
a	bond interaction parameter (Å)
b, c, d	dimensionless parameters
f	force on a cell (pN)
f_b	force on a bond (pN)
f_m	force at which cells detach most frequently (pN)
f_{50}	force at which 50% of the cells detach (pN)
h	height of confinement region
K_a	association constant or binding affinity (μm^2)
K_d	dissociation constant (μm^{-2})
k_B	Boltzmann's constant
k_f	forward reaction rate ($\mu m^2/s$)
k_r	reverse reaction rate (s^{-1})
m_l	surface density of ligands (μm^{-2})
m_{max}	max (m_r, m_l)
m_{min}	min (m_r, m_l)
m_r	surface density of receptors (μm^{-2})
n	number of bonds mediating adhesion
P_a	probability of adhesion
P_d	cumulative probability for an adherent cell to be detached
p_d	probability density of an adherent cell to be detached
p_n	probability of having n bonds
RCF	relative centrifugal force (g's)
T	temperature (K)
V	cell volume (μm^3)
$\langle\rangle$	average

Greek symbols

$\Delta\rho$	density difference between cell and medium
χ^2	weighted sum of square of errors
χ^2_ν	reduced weighted sum of squares of errors

INTRODUCTION

Cell-cell and cell-substrate adhesion is an integral component of many biological processes. The adhesive interaction is mediated by cell adhesion receptors binding specifically with their counter-receptors or ligands to form noncovalent bonds. An important parameter that characterizes such interaction at equilibrium is the binding affinity, K_a, which describes the propensity of a receptor-ligand pair to be in the bound state.

Traditional bulk chemistry approaches for measuring binding affinity were developed for binding of soluble ligands, such as cytokines or growth factors, to cell surface receptors. As such, these methods require at least one of the molecular species to be in solution (Hulme and Birdsall, 1992). This kind of binding affinity is referred to as three-dimensional (3D) affinity in the present paper, as the soluble ligands are able to move in three dimensions and there is no externally applied force acting on the bond. (Some authors use 3D affinity to describe the situation when both reactants are soluble (see Lauffenburger and Linderman, 1993).) In the case of cell adhesion, in contrast, the motions of both molecular species are restricted to two dimensions (2D), because both receptor and ligand are anchored to a surface. This kind of binding affinity is referred to as 2D affinity (Lauffenburger and Linderman, 1993). In addition, dislodging forces usually exist that affect the binding reaction. This coupling between chemistry and mechanics requires that the binding affinity be a function of the applied force instead of a constant value (Bell et al., 1984; Dembo et al., 1988). Because of these differences, the 3D affinity measured via

Received for publication 24 April 1997 and in final form 22 September 1997.

Address reprint requests to Dr. Cheng Zhu, School of Mechanical Engineering, Georgia Institute of Technology, Atlanta, GA 30332-0363. Tel.: 404-894-3269; Fax: 404-894-2291; E-mail: cheng.zhu@me.gatech.edu.

0006-3495/98/01/492/22 $2.00

traditional approaches may not be directly applied to the analysis of receptor-ligand binding in cell adhesion.

In a recent work, Dustin et al. (1996) measured the fluorescent intensities inside (total) and outside (free) the adhesion area and attributed the difference between the two as the density of the fluorescein isothiocyanate (FITC)-labeled LFA-3 (lymphocyte function associated antigen 3) receptors bound to the CD2 (cluster of differentiation 2) ligands. Using the Scatchard analysis, these authors determined the 2D dissociation constant of binding between LFA-3 reconstituted into glass-supported lipid bilayers and CD2 expressed on the Jurkat T cells that were free of dislodging forces. This work exemplifies the reasons behind the lack of methods for the direct measurement of binding affinity when both receptor and ligand are bound to apposing surfaces. Scatchard analysis is based on the definition of affinity as the concentration ratio of the bound to the free receptors and ligands, and it thus requires the ability to measure these concentrations separately. In adhesion assays, by contrast, only the fractions of adherent and detached cells are measured. Whereas there are no bonds associated with a detached cell, the number of bonds of an adherent cell can be any number allowable by the receptors and ligands in the contact area available for binding. The only (indirect) method we could find in the open literature for measuring density of bonds bridging two apposing surfaces is that of Dustin et al. (1996); and it requires that the receptor be freely mobile and that both the binding kinetics and lateral diffusion have reached equilibrium.

At the cellular level, adhesions are usually measured by either the probability or the strength of adhesion, which in population studies translate, respectively, into the fraction of adherent cells or the force dependence of the detached fraction of cells. Because cell adhesion is mediated by the formation of receptor-ligand bonds, and as such the adhesion probability and strength must relate to the force dependence of binding affinity of the adhesion molecules, the molecular binding characteristics could conceivably be derived directly from the cellular adhesion data. Here we report such a method. It consists of an experimental assay used to generate the adhesion data for various conditions and a theoretical model for the experiment. The assay employs centrifugation to detach less adherent cells. It is simple and widely used (McClay et al., 1981). However, although quantitative data could be generated by this technique (Chu et al., 1994), no theory exists in the literature that allows for their quantitative analysis to derive intrinsic properties of the adhesion molecules. Our mathematical model fills this gap. It derives from the probabilistic formulation for kinetics of small systems (McQuarrie, 1963) a simple but exact solution that relates the fraction of cells adhered to the number of bonds formed. The combination of the model and assay thus provides the means for measuring the force dependence of the 2D binding affinity.

The method was exemplified and validated experimentally by using a system that consisted of recombinant E-selectin-coated surface and carbohydrate ligand-expressing tumor cells. This greatly simplified system provides controls on the isolated adhesion pathway and the density of the receptor. E-selectin is a member of the selectin family of cell adhesion molecules that has been demonstrated to be important to the rolling of leukocytes on endothelial cells in sites of inflammation (Bevilacqua et al., 1987; Butcher, 1991; Lasky, 1992). It has also been implicated in mediating the adhesion of cancerous cell lines to endothelial cells in in vitro models of tumor metastasis (Rice and Bevilacqua, 1989; Sawada et al., 1993). Therefore, two well-characterized human cell lines whose adhesion to endothelium is mediated at least in part, by E-selectin, the promyelocytic leukemia cell HL-60 (Takada et al., 1993) and the colon carcinoma cell Colo-205 (Daneker et al., 1996), were chosen in the present study. The ability of selectins to mediate cell rolling is believed to be due to their binding characteristics, including the fast kinetic rates and the weak dependence of reverse rate on force (Kaplanski et al., 1993; Alon et al., 1995). Although the static centrifugation assay employed in the present study does not permit separate measurements of the forward and reverse kinetic rates, k_f and k_r, it allows the evaluation of their ratio, the binding affinity, $K_a = k_f/k_r$. In addition, the bond interaction parameter, a parameter that relates the reverse rate to bond force, can be obtained by the method developed herein. Both properties measured in the present work were consistent with those estimated with the flow chamber technique (Kaplanski et al., 1993; Alon et al., 1997).

The coupling between mechanics and chemistry in the interactions between cell-bound receptors and ligands is defined by the relation between the kinetic rates or binding affinity and the bond force, and several functional forms have been proposed (Bell, 1978; Bell et al., 1984; Dembo et al., 1988; Dembo, 1994; Evans et al., 1991; Evans, 1995; Evans and Ritchie, 1997). Although careful physical reasoning was used in their construction, the lack of detailed information regarding the binding pocket at the atomic level has prevented discrimination among these possible models based solely on theoretical grounds. The large amount of data generated via the centrifugation assay enabled us to test the applicability of these models to a specific receptor and ligand pair of physiological importance, i.e., the E-selectin and carbohydrate ligand system.

Our approach also allowed us to address several issues of importance to the biophysics of cell adhesion. These include the strength of cell adhesion, its relation to the probability of adhesion, the number of bonds per adherent cell, as well as the relationship between the adhesion strength and the binding affinity or the bond range. Our data suggest that Colo-205 cell adhesion to an E-selectin-coated surface was mediated by a small number (<5) of bonds. The dependence of adhesion strength on binding affinity was stronger than the logarithmic relation proposed in previous work (Dembo et al., 1988; Zhu, 1991; Kuo and Lauffenburger, 1993).

MATERIALS AND METHODS

Cell lines and antibodies

Colon carcinoma cells (Colo-205) were the generous gift of Dr. George Daneker (Emory University). Promyelocytic leukemia cells (HL-60) cells were obtained from American Type Cell Culture (ATCC, Rockville, MD). Both human cell lines were cultured in Roswell Park Memorial Institute (RPMI) 1640 media (Sigma, St. Louis, MO) supplemented with 2 mM L-glutamine, 100 units/ml penicillin, 10 mg/ml streptomycin, 0.25 μg/ml amphotericin B, and 10% fetal bovine serum (FBS). The anti-E-selectin monoclonal antibodies (mAbs) 1D6 (for capture) and 3B7 (for adhesion blockade) (Erbe et al., 1992), and the E-selectin construct (Lec-EGF, composed of the N-terminal lectin-like domain and the epidermal growth factor domain; Li et al., 1994) were gifts from Drs. D. Burns, B. Wolitzky, and K. S. Huang (Hoffmann-LaRoche, Nutley, NJ). The anti-sialyl Lewis x (sLe^x) mAb CSLEX1 was purchased from Becton Dickinson (San Jose, CA). The control antibody anti-ICAM-1 (intercellular adhesion molecule 1) mAb (84H10) was a gift of Dr. Steven Shaw (National Institutes of Health), and the anti-CD44 mAb (A3B8) was a gift of Dr. Barton Haynes (Duke University).

Coating wells with E-selectin construct

E-selectin was coated onto plastic wells by a capture protocol using the anti-E-selectin mAb 1D6 (Li et al., 1994). Plastic wells of 96-well plates (Immulon 2 Removawell Strips; Dynex, Chantilly, VA) were coated with either 1D6 or bovine serum albumin (BSA) (for control experiments) at 2–3 μg/ml in 100 μl of coating buffer (15 mM Na_2CO_3, 35 mM $NaHCO_3$ in H_2O) overnight at 4°C. The wells were washed two times with phosphate-buffered saline (PBS), 200 μl/well, and then blocked with blocking buffer (1% BSA in PBS without calcium and magnesium) overnight at 4°C. The E-selectin construct was then coated onto the plate at various concentrations diluted in RPMI 1640 medium with 1% BSA, 0.02% sodium azide overnight at 4°C.

Determination of E-selectin site density

The surface densities of E-selectin were determined via radioimmunoassays. Samples of the E-selectin construct were labeled with ^{125}I by using Iodo-Beads (Pierce, Rockford, IL). The specific activity was determined by measuring the activity of a known amount of protein. The radiolabeled E-selectin was used to coat the wells as described above. After coating, the wells were washed twice with RPMI 1640 with 1% BSA, 0.02% sodium azide to remove any unbound construct. The wells were then placed in a gamma counter to measure the activity present on the surface. The amount of E-selectin construct present was calculated by dividing the measured activity on the well by the specific activity of the labeled construct. The density of molecules was then calculated by converting the mass present on the well to number of molecules (molecular mass 25 kDa) and then dividing by the coated well area.

Centrifugation experiment

The target cells (Colo-205, HL-60) were radiolabeled by incubating with ^{51}Cr isotope (~150 μCi/10^6 cells) the night before the experiment. Colo-205 were detached from the culture flask with Hanks' balanced salt solution (Sigma) and 5 mM EDTA (Sigma) immediately before the experiment. HL-60 cells were grown in suspension and did not require detachment. Cells were washed twice in RPMI 1640 with 1% BSA (Sigma) to remove any radioactivity not associated with the cells. They were then suspended in RPMI 1640 with 1% BSA for the centrifugation experiment.

The target cells were added to the wells of 96-well plates at a concentration of 20,000–40,000 cells per well in a volume of 100 μl. The radioactivity of cells added in a sample was measured. The well strips (in a strip holder) were placed in a refrigerated centrifuge and spun at low speed (~8g for 30 s) to bring all cells into contact with the coated bottom surface. The wells were then incubated at 4°C for 30 min unless specified otherwise. After incubation, the wells were filled with medium and sealed to form an air-free system. The plates were then inverted and spun in the centrifuge to impose a defined force on the cells for a duration of 1 min unless specified otherwise. While the wells were kept inverted, the sealant strip was removed and the wells were drained of medium. The wells of the strip were separated, and the activity of each well was measured in a gamma counter. The fraction of adhesion was calculated by $P = (C_a - C_b)/(C_t - C_b)$, where C_a, C_b, and C_t are, respectively, the adherent, background, and total counts read by the gamma counter (TM Analytic, Brandon, FL).

Data analysis

The theoretical model was fitted to the experimental data by using a numerical routine that employs the Levenberg-Marquart method to evaluate the parameters that minimize the error (χ^2) between the data and the predictions (Press et al., 1989). The program also uses the spread and standard deviation of the data to estimate the standard deviations of the fitted parameters. The routine was set up for a two-parameter fit. When best fitting values of three parameters were desired, the third parameter was systematically varied and the two-parameter routine was applied for each value of the third parameter until the minimum χ^2 was found. The χ^2 statistic, or weighted sum of square of errors, was defined by

$$\chi^2 \equiv \sum_{i=1}^{N} \left\{ \frac{1}{\sigma_i^2} [y_i - y(x_i)]^2 \right\}$$

where y_i is the measurement at x_i; $y(x_i)$ is the model prediction at x_i; σ_i is the standard deviation of y_i at x_i; and N is the number of data points. The reduced χ^2 statistic, $\chi_\nu^2 = \chi^2/\nu$, where ν is the number of degrees of freedom ($= N - M$, where M is the number of fitting parameters), is both a measure of the appropriateness of the proposed model and a gauge of the quality of the data (Bevington and Robinson, 1992). To examine the goodness of fit of various models, the χ_ν^2 values were compared among different models for the same data set. To evaluate the quality of the data among various experimental runs, the χ_ν^2 statistics were again compared among different data sets for the same model.

THEORY

The master equations

As discussed in the Introduction, the traditional approaches to determining 3D binding affinity are inapplicable to the 2D case because of the lack of methods for directly measuring the densities of bonds in the contact area. Therefore, the key to the present approach is to relate the binding affinity to the measured fractions of adherent and detached cells and to infer the bond density from these fractions. Accomplishing this requires a model for cell detachment. In formulating such a model, it is important to realize that, when a population of cells is assayed, it is usually a fraction, not all or none of the cells, that are adherent. The fraction of adherent cells decreases with decreasing receptor and/or ligand densities and with increasing dislodging force.

To account for this lack of all-or-none, or indeterministic, phenomenon requires a hypothesis of its underlying random events. Two such hypotheses were proposed, one at the molecular and the other at the cellular level. The latter (model II) concerns the heterogeneity of a cell population

and is dealt with in the Appendix. The former (model I) postulates that the adhesion fractionalization is a manifestation of the stochastic nature inherent in receptor-ligand binding, which becomes significant when the number of bonds per cell is small. Therefore, the master equations for kinetics of small systems (McQuarrie, 1963) were adopted to describe the rate of changes in probabilities, p_n, of a cell having n bonds with another cell or surface,

$$\frac{dp_n}{dt} = (n+1)k_r^{(n+1)}p_{n+1} - \left[(A_c m_r - n)(A_c m_l - n)\frac{k_f^{(n+1)}}{A_c} + nk_r^{(n)}\right]p_n + [A_c m_r - (n-1)][A_c m_l - (n-1)]\frac{k_f^{(n)}}{A_c}p_{n-1} \quad (1)$$

where n ranges from 0 to $A_c m_{min}$ and p_n are zero for n values outside this range. A_c (in μm^2) is the contact area. $m_{min} = \min(m_r, m_l)$, where m_r and m_l (in sites/μm^2) are, respectively, the densities of receptors and ligands. The assumptions underlying Eq. 1 are that the probabilities at the current time point depend only on their immediate past, but not the history before that (i.e., the process of bond formation and breakage is Markovian); that the probability of simultaneously forming or breaking more than one bond at a time is infinitesimal compared to that of forming or breaking one bond at a time; that all free receptors and ligands within the contact area have equal opportunities to form a bond; and that every bond has the same probability of dissociating.

Constitutive equation for binding affinity

Following Cozens-Roberts et al. (1990), the master equations (Eq. 1) incorporate the coupling of the mechanics of the separation force with the chemistry of the kinetic rate coefficients. The forward ($k_f^{(n)}$; in μm^2/s) and reverse ($k_r^{(n)}$; in 1/s) rate coefficients for formation and breakage of the nth bond, respectively, are assumed to depend on the bond force, f/n, where f is the dislodging force acting on the cell, which is assumed to be equally shared by all (n) bonds. Because the centrifugation experiment used in this work only allows determination of the ratio of $k_f^{(n)}$ to $k_r^{(n)}$ but not each of them separately, we are only concerned with the binding affinity (equilibrium coefficient), for which the following functional form is proposed:

$$K_a\left(\frac{f}{n}\right) \equiv \frac{k_f^{(n)}}{k_r^{(n)}} = K_a^0\left[1 + c\left(\frac{af}{nk_BT}\right)^d\right]^{-1}\exp\left[-\left(\frac{af}{nk_BT}\right)^b\right] \quad (2)$$

where K_a^0 (in μm^2) is the affinity in the absence of force (zero-load affinity), k_B is the Boltzmann constant, and T is the absolute temperature. a (in Å) can be viewed as the range of the energy well that defines the bound state; it is referred to as the bond interaction parameter. k_BT/a provides a reference scale for the bond force. b–d are dimensionless parameters. Bell et al. (1984) suggested the inclusion of the bond elastic energy (in its simplest linear spring form) in the Gibbs free energy change of the binding reaction in the absence of force. This corresponds to the case of $b = 2$ and $c = 0$ in Eq. 2; and $k_BT/2a^2$ is the spring constant. Dembo (Dembo, 1994; Dembo et al., 1988) suggested two exponential laws for $k_f^{(n)}$ and $k_r^{(n)}$, but required their ratio to satisfy the equation of Bell et al. (1984) for K_a. Other authors have adapted Bell's (1978) exponential model for $k_r^{(n)}$, but assumed $k_f^{(n)}$ to be a constant (Hammer and Lauffenburger, 1987; Cozens-Roberts et al., 1990). This is the $b = 1$ and $c = 0$ case in Eq. 2. Evans (Evans, 1995; Evans et al., 1991) proposed a power law for $k_r^{(n)}$ (with $k_f^{(n)}$ assumed constant, this becomes the $b = 0$, $c = 1$ case in Eq. 2) and described the bonds as brittle if the power $d \gg 1$ and ductile if $d \approx 1$. (Evans' original form was $k_r(f/n) = k_r^0(af/nk_BT)^d$, and hence $k_r(0) = 0$. Our modified version includes a cross-over to a nonzero reverse rate at zero force.) More recently, Evans and Ritchie (1997) placed the relationship between reverse rate and bond force on a more rigorous foundation by deriving it from Kramers' (1940) theory of escape of thermally agitated particles from an energy well tilted by an applied force. Under greatly simplified conditions, the result obtained by Evans and Ritchie (1997) was a combined power and exponential model (i.e., $c = 1$ and nonzero b and d values, again with $k_f^{(n)}$ assumed constant). Although their ranges have been estimated, the model parameters cannot be determined theoretically, because no information is available for the receptor/ligand in question, on either the detailed energy profile that determines the transition state or the work mode that couples the external force to energy. Here Eq. 2 is viewed as a constitutive equation for the binding affinity whose parameters will be evaluated from comparison to experiment.

Exact steady-state solution

Although in its general form, Eq. 1 can be used to describe transient adhesion (Piper, 1997), only the steady state is relevant to the centrifugation experiment described herein. Using mathematical induction, we were able to solve exactly the system of finite-difference equations resulted from setting the left-hand side of Eq. 1 to zero. This closed-form solution, which can be directly verified upon substitution into Eq. 1 (Piper, 1997), reads

$$p_n(f) = \frac{p_0(f)}{A_c^n}\binom{A_c m_r}{n}\binom{A_c m_l}{n}\prod_{i=1}^{n} iK_a\left(\frac{f}{i}\right) \quad (3a)$$

where the probability of a cell having no bond (detached) can be obtained via normalization, $\sum_0^{A_c m_{min}} p_n = 1$, which

leads to

$$p_0(f) = \left[1 + \sum_{n=1}^{A_c m_{min}} \binom{A_c m_r}{n} \binom{A_c m_l}{n} A_c^{-n} \prod_{i=1}^{n} iK_a\left(\frac{f}{i}\right)\right]^{-1} \quad (3b)$$

As expected, the steady-state solution (Eq. 3) no longer depends on the forward and reverse rate coefficients separately but on their ratio, the binding affinity, as a whole. It should be noted that the general mathematical structure of this solution depends only on the definition of the binding affinity (Eq. 2), but not on its specific functional form (e.g., that given by the far right-hand side of Eq. 2). Therefore, its application includes, but is not limited to, systems described by such a functional form.

Two simplified cases

When one of the molecular species excessively outnumbers the other, the density of the former can be approximated as constant because the reaction is limited by the availability of the latter. As such, the kinetic mechanism can be reduced to one of a first-order reversible reaction between free and bound states of the limiting species. The master equations for this simplified binding mechanism can be obtained from Eq. 1 by replacing $(A_c m_{max} - n)$ and $[A_c m_{max} - (n - 1)]$ by $A_c m_{max}$, where $m_{max} = \max(m_r, m_l)$. Such simplified master equations were used by Cozens-Roberts et al. (1990). The steady-state solution is reduced to

$$p_n(f) = p_0(f)\binom{A_c m_{min}}{n} \prod_{i=1}^{n} m_{max} K_a\left(\frac{f}{i}\right) \quad (4a)$$

where

$$p_0(f) = \left[1 + \sum_{n=1}^{A_c m_{min}} \binom{A_c m_{min}}{n} \prod_{i=1}^{n} m_{max} K_a\left(\frac{f}{i}\right)\right]^{-1} \quad (4b)$$

As can be seen, the affinity for the simplified mechanism should be $m_{max}K_a$.

When the number of bonds having nonvanishing probabilities is much smaller than both the numbers of receptors and ligands in the contact area available for binding, the formation of a small number of bonds will not significantly deplete the free receptors and ligands. As such, the system of master equations can be approximated by one that neglects, respectively, n and $(n - 1)$ in $(A_c m_i - n)$ and $[A_c m_i - (n - 1)]$ (subscript $i = r$ or l) in Eq. 1, which was employed by Kaplanski et al. (1993). The steady-state solution to the reduced equations is

$$p_n(f) = p_0(f) \prod_{i=1}^{n} \frac{1}{i} A_c m_r m_l K_a\left(\frac{f}{i}\right) \quad (5a)$$

where

$$p_0(f) = \left[1 + \sum_{n=1}^{A_c m_{min}} \prod_{i=1}^{n} \frac{1}{i} A_c m_r m_l K_a\left(\frac{f}{i}\right)\right]^{-1} \quad (5b)$$

As can be seen, the per-molecule density binding affinity K_a appears in Eq. 5, together with the densities of the receptors and ligands, as well as the contact area as a grouped quantity, i.e., the per-cell binding avidity $A_c m_r m_l K_a$.

Note that, if $f = 0$, Eqs. 4b and 5b reduce, respectively, to $p_0(0) = (1 + m_{max}K_a^0)^{-A_c m_{min}}$ and $p_0(0) = \exp(-A_c m_r m_l K_a^0)$. Thus the binomial and Poisson distributions are recovered from Eqs. 4a and 5a, respectively, by setting $f = 0$. This is not surprising, as the conditions underlying these distributions are equivalent to the assumptions on which the master equations and their corresponding simplifications are based. Both distributions have been suggested by others to describe the formation of a small number of bonds (Bell, 1981; Capo et al., 1982; Evans, 1995). However, these previous works assumed the parameters involved as given. In contrast, our closed-form solutions reveal how these parameters are related to the binding affinity, the contact area, and the densities of receptors and ligands. In the binomial distribution, the probability that a receptor will bind a ligand is $p = [1 + (m_{max}K_a^0)^{-1}]^{-1}$. In the Poisson distribution, the average number of bonds is $\langle n \rangle = A_c m_r m_l K_a^0$. In addition, our derivation of these distributions from the master equations enabled their generalization to the case in which the bonds are stressed (i.e., when $f \neq 0$) and the simplifying assumptions are removed (i.e., when $\langle n \rangle$, $A_c m_r$, and $A_c m_l$ are comparable).

Relating the strength to the probability of adhesion

The probability and the strength of cell adhesion have been regarded as two separate physical quantities (Bongrand et al., 1982). The coupling of mechanics and chemistry via the force dependence of binding affinity (Eq. 2) allows the two to be related. For the small systems under consideration, the deterministic notion of adhesion strength, defined as the force required to detach an adherent cell, is no longer applicable and needs to be extended. The reason is that, in the present probabilistic framework, the detachment of a given cell is a random event and hence can happen at any force, even at zero force. It is this stochastic nature of the individual cell detachment that is assumed to give rise to the fractionalization of adhesion seen in a population of cells. However, the probability of adhesion, defined as the probability of a cell having at least one bond, is predictable and decreases with the applied force:

$$P_a = 1 - p_0 \quad (6a)$$

where p_0 is given by Eq. 3b, 4b, or 5b. The probability of an initially adherent cell (i.e., adherent when $f = 0$) remaining adherent after it is subjected to a force is $P_a(f)$, renormal-

ized by $P_a(0)$ to discount the initially nonadherent cells. The cumulative probability that an adherent cell will be detached by a force not exceeding f is therefore

$$P_d(f) = 1 - P_a(f)/P_a(0) \tag{6b}$$

The probability density that an adherent cell will be detached by an applied force can be obtained by differentiating Eq. 6b:

$$p_d(f) = \frac{dP_d}{df} \tag{6c}$$

This in general is a broad distribution. There is no one force at which a cell will shift abruptly from adherent to nonadherent. Nevertheless, various statistical definitions for the strength of cell adhesion can be obtained. Three possible definitions are: f_m, the force at which detachment occurs most frequently; f_{50}, the force at which 50% of the adherent cells have been detached; and $\langle f \rangle$, the average force required to detach an adherent cell. These are given by, respectively,

$$\frac{dp_d(f_m)}{df_m} = 0 \qquad P_d(f_{50}) = 50\% \qquad \langle f \rangle = \int_0^\infty f p_d(f) df \tag{7a–c}$$

which correspond, respectively, to the mode, median, and mean of the probability distribution $p_d(f)$.

Relation to deterministic affinity

The analytical solutions for the probability distribution of having bonds (Eqs. 3–5) also enable one to calculate various statistical aspects, including the mean, $\langle n \rangle$, and variance, σ_n^2 ($= \langle n^2 \rangle - \langle n \rangle^2$), of the bond number. It follows from direct calculations of $\langle (A_c m_r - n)(A_c m_l - n) \rangle$ that (Piper, 1997)

$$\frac{\langle n \rangle}{\left\langle n/K_a(f/n) \right\rangle} = \frac{\langle n \rangle / A_c}{(m_r - \langle n \rangle / A_c)(m_l - \langle n \rangle / A_c) + \sigma_n^2 / A_c^2} \approx \frac{\langle n \rangle}{m_{max}(A_c m_{min} - \langle n \rangle)} \tag{8}$$

where the far right-hand side corresponds to the simplified case where one of the molecular species excessively outnumbers the other. This is an interesting result because it reveals how the binding affinity (defined by Eq. 2 as the ratio of forward to reverse rate coefficients based on the detailed balance between formation and breakage of small number of bonds for each n value) is related back to its traditional deterministic definition for large systems. $\langle n \rangle / A_c$ in Eq. 8 can be readily identified as the deterministic bond density in the large system limit. In general, statistical fluctuations (as measured by the standard deviation σ_n) become smaller as the system becomes larger. Thus the right-hand side of Eq. 8 approaches, as $\langle n \rangle \to \infty$, the deterministic definition of binding affinity, which is the density ratio of bonds to free receptors and ligands.

If $f = 0$, the left-hand side of Eq. 8 is equal to K_a^0 (according to the far right-hand side of Eq. 2). If $f \neq 0$, the left-hand side of Eq. 8 can be viewed as a weighted statistical average of the stressed binding affinity over all subpopulations of cells that are adhered via different numbers of bonds and hence have different binding affinities. It is expected that this weighted average will approach $K_a(f/\langle n \rangle)$ as $\langle n \rangle \to \infty$.

RESULTS

Quantification of E-selectin site density

The densities of immobilized E-selectin were well correlated with the concentrations of E-selectin construct used to coat the wells (Fig. 1). The fitted calibration curve was then used to predict, based on the concentrations of the E-selectin construct in the coating solutions, its surface number densities in the centrifugation experiments. Because the capture antibody binds to an epitope on the E-selectin construct that is away from the lectin binding domain (Erbe et al., 1992), it was assumed that all E-selectin molecules captured by the 1D6 were properly oriented.

Confirmation of binding specificity

Specificity was demonstrated in Fig. 2, which showed that both target cells adhered to wells coated with E-selectin but not to those coated with BSA or 1D6 alone. Furthermore,

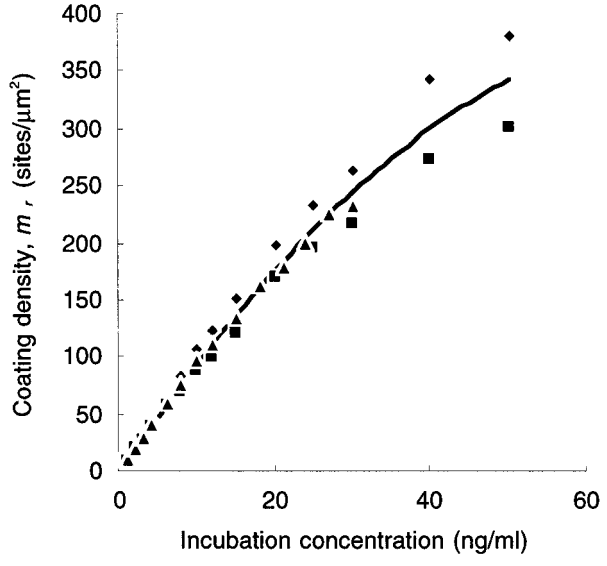

FIGURE 1 Correlation between concentrations of E-selectin construct used to coat the plate and its densities coated on the surface, as determined by radioimmunoassays. The data represent the combined results of three separate experiments, as indicated by different symbols (◆, ■, ▲). Each point represents the mean of four wells. The standard deviations are omitted for clarity, but they are of the same size as the symbols. The continuous curve was a quadratic fit to the data.

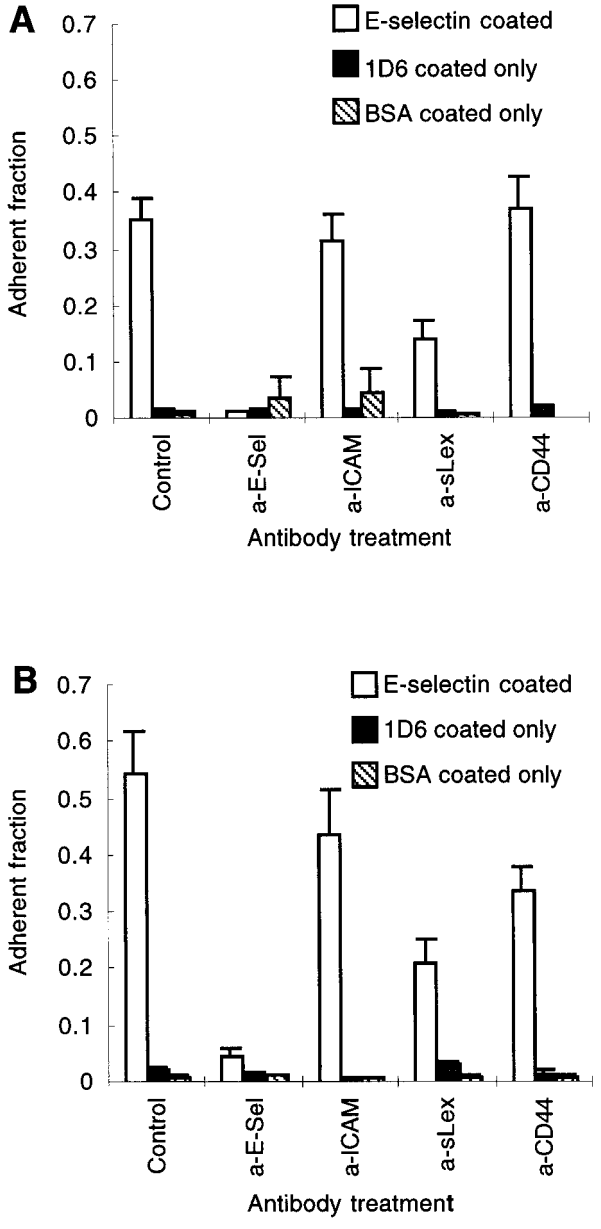

FIGURE 2 Demonstration of specificity of target cell adhesion to the E-selectin-coated wells. Both Colo-205 cells (*A*) and HL-60 cells (*B*) adhered to E-selectin-coated wells (□), but not to wells coated with BSA (▨) or the capture antibody 1D6 only (■). Adhesion to the E-selectin-coated wells was abolished by incubation of the wells with an anti-E-selectin mAb, 3B7, whereas incubation with an irrelevant isotype-matched anti-ICAM mAb did not affect adhesion. Incubation of the target cells with an anti-sLe^x mAb (CSLEX1) also decreased adhesion from control levels, although the blockade was incomplete. In contrast, incubation with an irrelevant isotype-matched anti-CD44 mAb did not significantly reduce adhesion. Data were presented as mean ± SD of six wells. The experiment was repeated twice, with similar results.

the anti-E-selectin mAb (3B7), but not the irrelevant isotype-matched mAb (anti-ICAM-1, 84H10), was able to block nearly 100% of binding to the E-selectin-coated wells. In addition, the anti-sLe^x antibody (CSLEX1), but not the irrelevant isotype-matched mAb (anti-CD44, A3B8), partially inhibited adhesion to E-selectin (by 50%). This incomplete blockade suggests that binding epitopes other than sLe^x (e.g., sLe^a) also contribute to adhesion (Springer, 1995). None of the antibodies had any effects on binding to the BSA- or 1D6-coated wells (Fig. 2). Assuming independence between specific and nonspecific bindings, the former (P_a) can be calculated from the latter (P_n) and total binding (P_t) as $P_a = (P_t - P_n)/(1 - P_n)$.

Testing the steady-state hypothesis

The closed-form solutions (Eqs. 3–5) require the adhesion process to have reached steady state. In addition to choosing E-selectin, which was thought to have very fast kinetics (Kaplanski et al., 1993; Alon et al., 1995; Puri et al., 1997), three types of experiments were designed to test the validity of this assumption. The first of these examined the effect of (or the lack thereof) contact duration on binding, in which adhesions under two conditions were compared. After being added to the wells and spun down by a low RCF (8*g*, 30 s), either the Colo-205 cells were allowed to incubate with the E-selectin-coated surface for 30 min, or without incubation, the plate was inverted and a high RCF (44*g*, 60 s) was applied to detach the less adherent cells. As shown in Fig. 3, comparable adhesions resulted from both conditions for eight different coating densities, as the ratios of adhesion fractions under the latter to the former conditions were not significantly different from unity. This suggests that, for the receptor-ligand system used, even the shortest contact duration (approximately tens of seconds) that could be

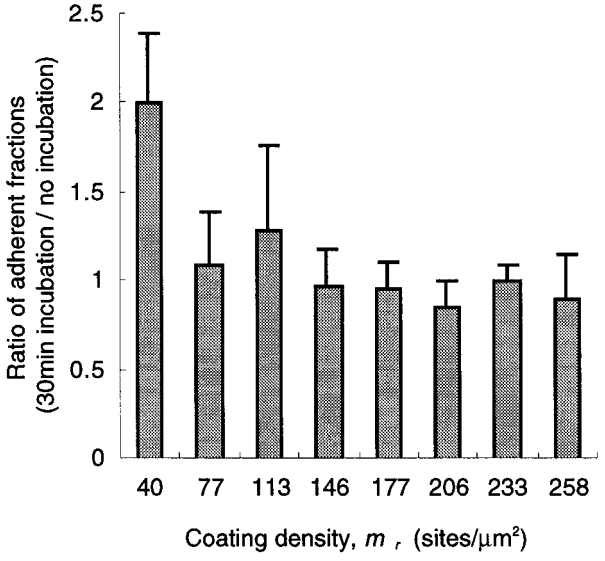

FIGURE 3 Lack of effect of incubation time on adhesion. Colo-205 cells were spun down into contact with the E-selectin-coated surface at a low speed, and were either immediately subjected to a RCF of 44*g* or allowed to incubate for 30 min at 4°C before centrifugation. The ratios of adhesions under the latter conditions to adhesions under the former conditions were plotted against various E-selectin coating densities. The data represent an average of at least five wells each of 30 min and no incubation per column. The error bars were calculated from standard deviations of both conditions.

achieved using the centrifugation technique was sufficiently long for the bond formation kinetics to reach steady state. It also supports the validity of the constant contact area assumption implied in the models.

In the second set of experiments, the effect on adhesion of (or the lack thereof) the duration of force application was examined. Colo-205 cells were spun down at low speed into contact with surfaces coated with E-selectin at ~200 sites/μm^2. After 30 min of incubation, cells were subject to a RCF of 44*g* for various times. As can be seen in Fig. 4 *A*, no correlation was found between the duration of applied force and cell detachment over the range of 1–15 min of spinning. This suggests that all cell detachment occurred before the shortest duration tested, after which continued application of the same constant force did not result in further detachment. Although it supported the steady-state assumption, this result was surprising, in view of the dynamic nature of chemical equilibrium and the short lifetime of E-selectin/carbohydrate bonds (Kaplanski et al., 1993; Alon et al., 1997). This point will be revisited in the Discussion.

The third set of experiments examined whether detachment depended on the history of force application. A direct consequence of the master equations (Eq. 1) is that their general transient solution at any given time depends on the entire history of the applied force before that time instead of just on its value at the current time. The steady-state solution (Eq. 3), however, depends only on the steady-state force but not on its history. Because detachment occurred at a very short time (preceding paragraph) and because the fraction of adhesion P_a is a monotonically decreasing function of force f (cf. Eqs. 3b and 6a), it was predicted that detachment should be dependent on only the maximum value in the ramp force history. This prediction was tested by accelerating the microprocessor-controlled centrifuge (Jouan, St. Herblain, France) at various rates while the maximum speed was kept constant. It is evident from Fig. 4 *B* that the time over which the centrifuge was accelerated (ranging from 10 to 80 s) had no significant effect on the adhesion fraction. This result further validated the steady-state assumption.

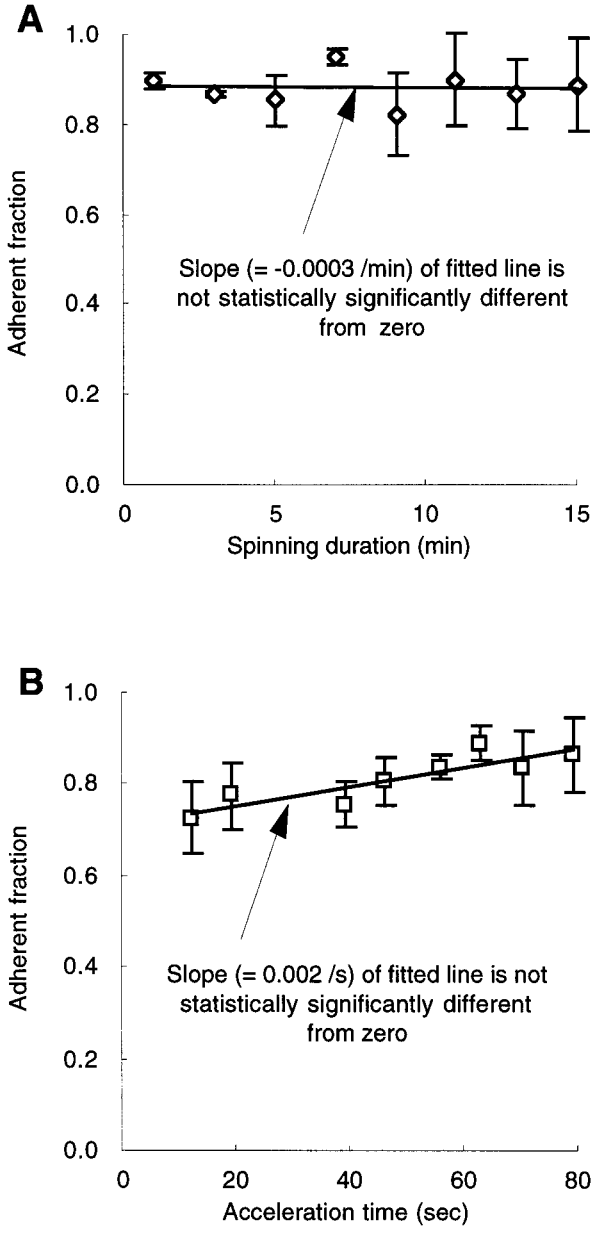

FIGURE 4 Lack of effect of (*A*) duration of force application and (*B*) acceleration rate on cell detachment. Adhesions of Colo-205 cells (to surface coated with ~200 sites/μm^2 E-selectin construct) were plotted against various time intervals, during which either (*A*) a constant RCF of 44*g* was applied (after a shortest possible acceleration period) or (*B*) the centrifuge was gradually accelerated to the same final speed (equivalent to 44*g*). Each data point represents the mean ± SD of six wells. Lines represent linear fit to the data. The slope of each fit, as indicated, is not significantly different statistically from zero.

Verification of the monovalency of E-selectin binding

Implicit in Eqs. 1 and 8 is the proposed kinetic mechanism for E-selectin/carbohydrate ligand binding as a second-order forward, first-order reverse, monovalent bimolecular reaction. It follows from the Taylor series expansion (cf. Eqs. 5b and 6a) that, when m_r or m_l is small,

$$P_a \approx A_c m_r m_l K_a(f) \tag{9}$$

This prediction was tested by measuring the dependence of adhesion on the E-selectin density. The results are shown in Fig. 5. As expected, the detached fraction increased with increasing centrifugal forces. For each given force value and over a wide range, the adherent fraction increased nearly linearly with the E-selectin density when it was low (Fig. 5 *A*), which supports the monovalency of the E-selectin binding (Alon et al., 1995). Binding became saturated when E-selectin density reached 100 sites/μm^2 (Fig. 5 *B*), which suggests a ligand density on the order of 100 sites/μm^2. However, it was not tested whether the ligand binding was also monovalent, because we did not change its density.

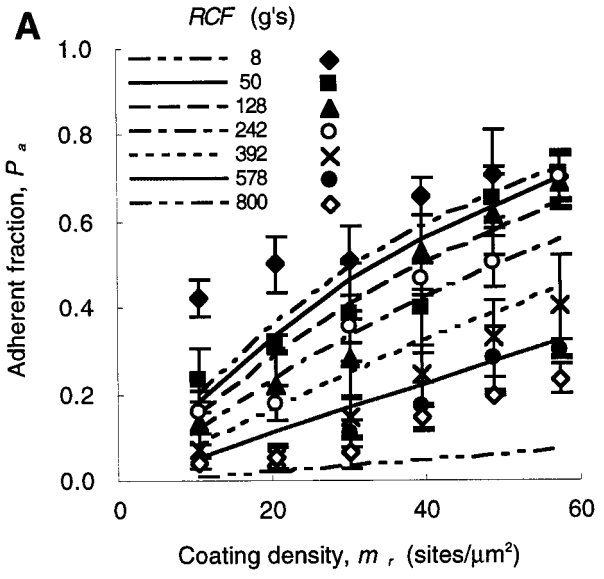

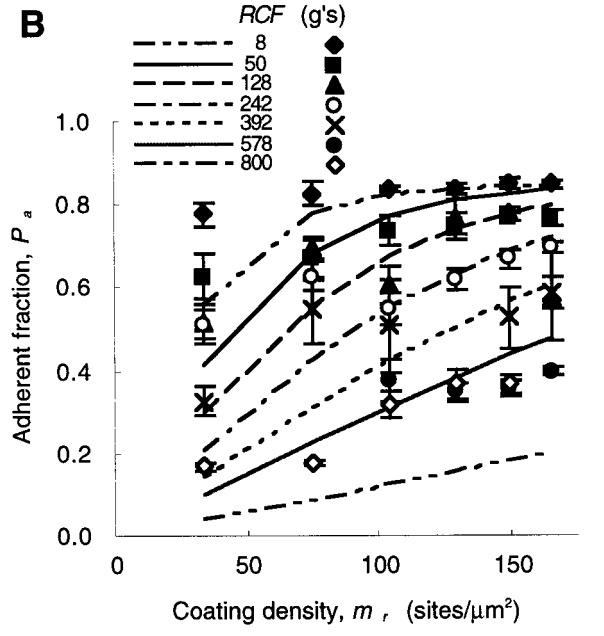

FIGURE 5 Dependence of Colo-205 cell adhesion on the E-selectin coating density (m_r) and relative centrifugal force (RCF). (*A*) Adhesion is nearly proportional to m_r at low E-selectin densities. (*B*) Adhesion is saturable at high densities of E-selectin. Curves are model predictions with parameter values $b = 1$, $c = 0$, $A_c m_l K_a^0 = 0.0236$ μm², $a = 0.157$ Å for *A*, and $b = 0$, $c = 1$, $d = 0.8$, $A_c m_l K_a^0 = 0.0644$ μm², $a = 3.4$ Å for *B*.

Direct measurement of $K_a(f)$

It follows from Eq. 9 that the ratio of P_a to m_r at any constant RCF is an approximation to the per E-selectin density cellular avidity, $A_c m_l K_a$, at the force level corresponding to that RCF. Thus the P_a/m_r versus f plot shown in Fig. 6 provides a direct measurement of the dependence of binding affinity on force. It should be pointed out that this result is predicted from the master equations, which are

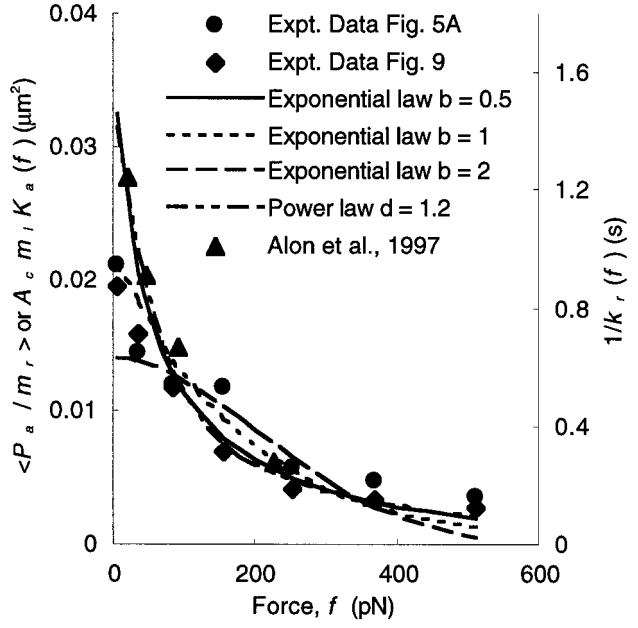

FIGURE 6 Relations between binding affinity (*left ordinate*) or reverse rate coefficient (*right ordinate*) and force on a cell (*abscissa*). The average ratio of adhesive fraction (P_a) to site density (m_r) for the points of the constant RCF curves shown in Figs. 5 *A* (●) and 9 (◆) are plotted against force on a cell that is produced at that RCF. Theoretical predictions (*curves*) made using various forms of the $A_c m_l K_a$ versus f relationship (Eq. 2) are also shown. The parameters (see Tables 1 and 2) were calculated by fitting the predictions of indicated model forms with the data shown in Fig. 9 instead of fitting data in this figure. Also shown for comparison are $1/k_r$ versus f data (▲), measured via flow chamber experiments (from Alon et al., 1997, by permission).

independent of the specific functional form for $K_a(f)$. Therefore it should be used to guide the construction of the constitutive equation, such as that given by the right-hand side of Eq. 2. It is worth noting that the P_a/m_r versus f data computed from two sets of data (one shown in Fig. 5 *A* and the other Fig. 9) are in very good agreement, attesting to the reliability of the results.

Validation of model predictions

The model was tested for its ability to describe an entire set of binding curves (P_a versus various RCF and m_r). Fig. 5 *A* shows the model prediction (*curves*), using a simple exponential law for the binding affinity with two fitting parameters ($A_c m_l K_a^0$ and a) and fixed values of $b = 1$ and $c = 0$ in Eq. 2. The data in Fig. 5 *B* were fitted using a power law formulation with three fitting parameters ($A_c m_l K_a^0$, a, and d; b was set equal to zero in Eq. 2). A detailed examination of the abilities of various models to account for the data will be presented shortly. Here, only two are shown to exemplify the comparison between the theory and the experiment. Not all of them represent the best model. They are shown to allow the readers via direct visual inspection to develop a sense of what the quantitative measure of the goodness of fit (χ_ν^2 in Tables 1 and 2) means. These reasonable fits should

TABLE 1 Model I parameters calculated using the exponential law ($b \neq 0$, $c = 0$)

Data sets shown in figure	No. of data points (N)	No. of fitting parameters (M)	Predicted model parameters ± estimated SD			Reduced chi square* χ_v^2
			b	$A_c m_l K_a^0$ (μm^2)	a (Å)	
5 *A*	41	3	0.6	0.0320 ± 0.0015	0.280 ± 0.017	2.3
		2	**1**	0.0236 ± 0.0009	0.157 ± 0.006	2.7
		2	**2**	0.0175 ± 0.0004	0.108 ± 0.006	5.4
5 *B*	40	3	0.4#	0.0511 ± 0.0018	1.240 ± 0.056	13.1
		2	**1**	0.0226 ± 0.0002	0.211 ± 0.004	21.6
		2	**2**	0.0175 ± 0.0003	0.139 ± 0.001	39.4
9	42	3	0.5	0.0445 ± 0.0028	0.775 ± 0.052	1.5
		2	**1**	0.0218 ± 0.0010	0.225 ± 0.008	2.3
		2	**2**	0.0140 ± 0.0005	0.142 ± 0.003	5.8

*See data analysis for definition of χ_v^2.
#Further reduction of b resulted in a slight reduction of χ_v^2, but gave an unreasonable value for a. Boldface indicates that the values were held constant during the fitting.

be appreciated, for a very small number of parameters were used in the curve fitting of such a large collection of data, ranging over six different E-selectin coating densities and seven levels of centrifugal forces.

In addition to fitting the entire collection of data with a single set of parameters, each subset of P_a versus RCF data (for a given m_r) in a third data set was used to evaluate the binding characteristics. The parameters so predicted ($A_c m_l K_a^0$ and a, for given values of $b = 1$ and $c = 0$) are plotted against the E-selectin site density, m_r, in Fig. 7. As can be seen, no dependence of the parameter values on m_r was found, supporting the validity of the model and indicating that these are indeed intrinsic parameters. In other words, the two model parameters evaluated by best fitting any one set of adhesion versus centrifugation force data in the family (for a given m_r) enabled us to accurately predict, without any fudge factor, other sets of P_a versus RCF data in the family (for other m_r values), as shown in Fig. 8.

When individual P_a versus m_r data (for a given RCF) were fitted to evaluate the binding characteristics, however, variations were seen (data not shown) in the predicted values of a at small RCF (e.g., 8g) values. Such a result pointed out a limitation of the method. Because the parameter a determines how the applied force influences adhesion, data generated from experimental situations where the separation force is low and does not play a significant role are not suited for its evaluation.

Comparison of various models for binding affinity

A key element of the model is the constitutive equation relating the binding affinity to force (Eq. 2). While different formulations for the reverse rate and/or affinity (as represented by different values for b and c in Eq. 2, with or without the additional assumption for constant forward rate) have been proposed by several authors (Bell, 1978; Bell et al., 1984; Dembo et al., 1988; Evans et al., 1991; Evans, 1995; Evans and Ritchie, 1997), their ability to account for any real receptor-ligand interaction data has not been compared experimentally. Using our data from the centrifugation experiment, we conducted such a comparative study. The results are summarized in Tables 1 and 2. The goodness of fit of the curves that resulted from using different models is quantified by the best fitting values of the reduced χ^2 statistic, χ_ν^2, which reflects both the appropriateness of the model and the quality of the data (Bevington and Robinson, 1992).

We first examined the exponential law (the $b \neq 0$, $c = 0$ case). It is evident from direct visual inspection that the exponent of $b = 1$ (Fig. 9 *A*) clearly represented our data better than that of $b = 2$ (Fig. 9 *B*). This conclusion holds true for all data sets (Table 1). The exponent b was also allowed to freely vary to arrive at a value that best fitted the data, which consistently yielded $b \approx 0.5$ (Fig. 9 *C*). Again, the χ_ν^2 at $b \approx 0.5$ was smaller than the χ_ν^2 at $b = 1$ for all sets of data summarized in Table 1.

TABLE 2 Model I parameters calculated using the power law ($b = 0$, $c = 1$, $d \neq 0$)

Data sets shown in figure	No. of data points (N)	No. of fitting parameters (M)	Predicted model parameters ± estimated SD			Reduced chi square* χ_v^2
			d	$A_c m_l K_a^0$ (μm^2)	a (Å)	
5 *A*	41	3	1.2	0.0273 ± 0.0013	0.350 ± 0.024	2.4
5 *B*	40	3	0.8	0.0644 ± 0.0047	3.40 ± 0.38	12.3
9	42	3	1.2	0.0332 ± 0.0023	0.720 ± 0.059	1.1

*See data analysis for definition of χ_v^2.

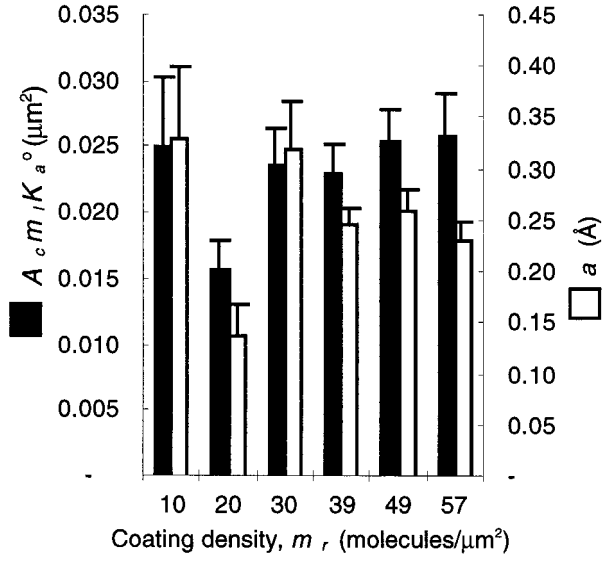

FIGURE 7 Independence of the fitted parameters on E-selectin site density. Each binding curve (one m_r but various RCFs) of the data in Fig. 7 was used to evaluate the best fitting parameters of $A_c m_l K_a^0$ (*solid bars, left ordinate*) and a (*open bars, right ordinate*), and the results were plotted against the E-selectin site density, m_r.

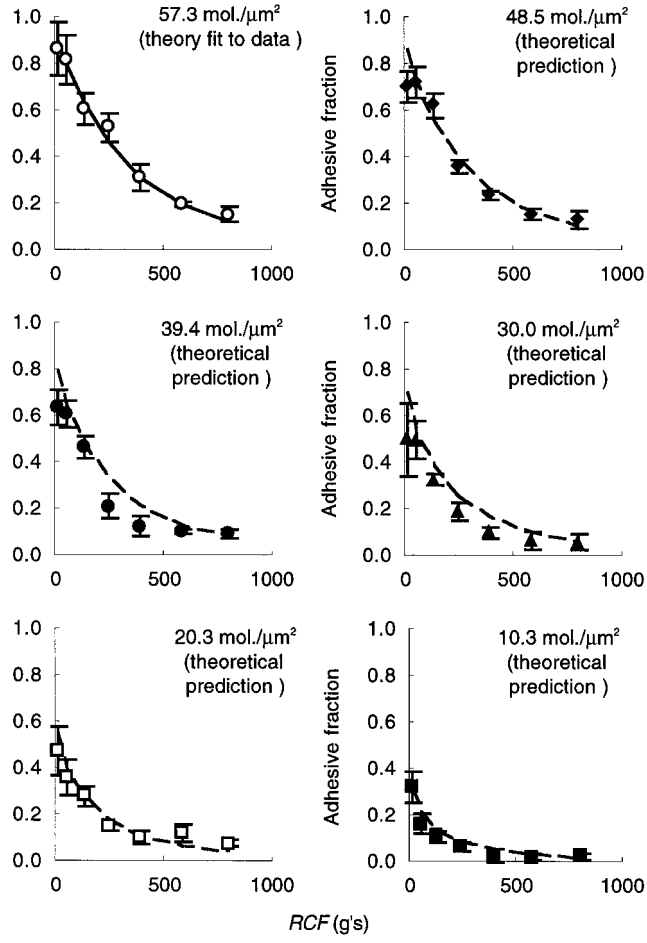

FIGURE 8 Prediction of adhesion behavior. Model I ($b = 0.5$, $c = 0$) was used to calculate the best fitting adhesion parameters ($a = 0.86$ Å, $A_c m_l K_a^0 = 0.055$ μm^2) based on the data shown in the upper left panel ($m_r = 57.3$ mol/μm^2). The model, with those calculated parameters, was then used to predict the adhesion behavior of the system when the different coating densities were used, which shows very good agreement between the theory (*curves*) and experiment (*points*).

The power law (the $b = 0$, $c = 1$ case) was next examined. That model fit the data (Fig. 9 *D*) slightly better than the exponential model with an equal number of free parameters ($M = 3$). This also holds true for all but one of the sets of data (Tables 1 and 2). The average best fitting d was ~1.1 (ranged from 0.8 to 1.2; Table 2), suggesting ductile bonds for the E-selectin/carbohydrate ligand interaction (Evans, 1995). The more general model (the $b \neq 0$, $c = 1$, $d \neq 0$ case) did not significantly reduce the χ_ν^2 value (not shown). Using this more complex model for our data appears not to be warranted, because the number of freely adjustable parameters was increased with no improvement in the goodness of fit.

The various functional forms of the K_a versus f relationship examined are plotted in Fig. 6 along with the P_a/m_r versus f data. It is evident that good agreement was found in such a comparison for the cases of $b = 0.5$ and $c = 0$, $c = 1$ and $d = 1.2$, as well as $b = 1$ and $c = 0$, and the discrepancy is significant for the model of $b = 2$ and $c = 0$, which are consistent with the χ_ν^2 results shown in Tables 1 and 2. It is worth mentioning that the theoretical curves, with parameters obtained from fitting of data of Fig. 9, fit both sets of data (the other set was computed from the data in Fig. 5 *A*).

Dependence of adhesion strength on binding characteristics

The binding affinity includes two parameters (for the exponential law with $b = 1$), i.e., the no-load binding affinity, K_a^0, and the bond interaction parameter, a. The dependence of the strength of cell adhesion on the former has been suggested to be of a logarithmic form (Dembo et al., 1988; Zhu, 1991; Kuo and Lauffenburger, 1993). Such a weak dependence was derived from thermodynamic models of cell adhesion (Dembo et al., 1988; Zhu, 1991), which required a large number of continuously distributed molecules for this prediction to be valid. It has not been examined whether such a logarithmic relationship would still hold true for adhesion processes that are mediated by a small number of discretely distributed molecules, as in the present case.

Using the model parameters evaluated from our experimental data, we computed the probability densities of detachment for Colo-205 cells from Eq. 6; these are shown in Fig. 10, *A* and *B*. Adhesion strength can be defined as f_m, f_{50}, or $\langle f \rangle$, via Eq. 7a–c, respectively. Also demonstrated in these figures is how the probability density of detachment is affected by the no-load binding affinity, K_a^0, and by the bond range, a. With all other parameters held constant, an increase in K_a^0 causes a rightward shift of the p_d versus f curve, indicating the ability of cells to remain adherent at greater dislodging forces (Fig. 10 *A*). The curve also changes shape

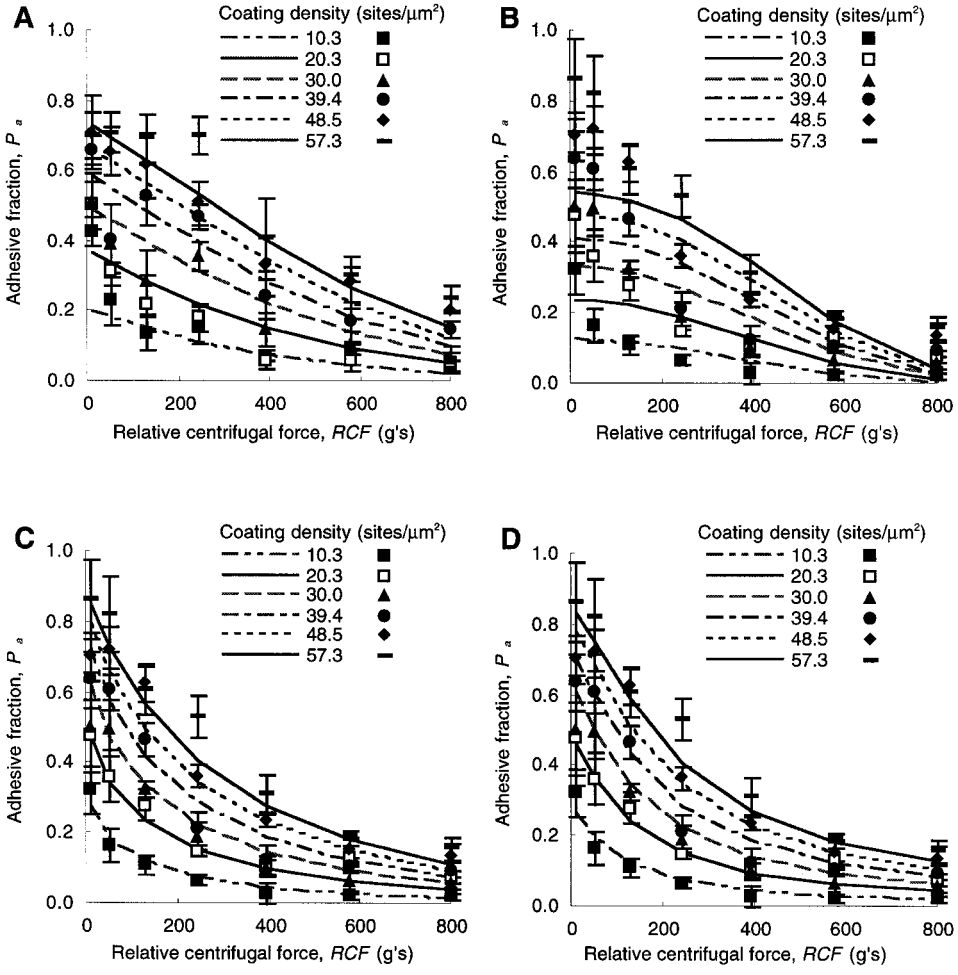

FIGURE 9 Comparison of the abilities of various special forms of Eq. 2 to account for the data. Differing forms of Eq. 2 were used in connection with Eqs. 3b and 6a to predict (*curves*) the same set of experimental data (*points*) using the best fitting parameter values (cf. Tables 1 and 2) to compare the appropriateness of their application. The exponential law ($c = 0$) with $b = 1$ (*A*) is a better model than that with $b = 2$ (*B*). If b is allowed to vary freely, then the best fitting value is $b \approx 0.5$ (*C*). The power law ($b = 0$, $c = 1$, and $d = 1.2$) also fits the data well (*D*).

as it is shifted to the right. It becomes bell shaped and less broadly distributed, which diminishes the differences of the three definitions of adhesion strength. This shift and change of shape resulted in a dependence of the adhesion strength on K_a^0, which is stronger than logarithmic. Such a relationship is plotted in Fig. 11 *A*.

The effect of the bond interaction parameter on the single bond strength was envisioned by Bell (1978), who argued how different values of a could alter the order of bond strengths based on the order of interaction energies. In the absence of forces, the high energy barrier a cell surface receptor has to overcome for it to escape from the membrane linkage ensures a stable anchor of the receptor for a seemingly infinitely long time, whereas the low binding energy of the receptor for a ligand results in spontaneous dissociation in an observable time. However, the force required to extract the receptor from the cell membrane is estimated to be on the same order of magnitude as that required to break a receptor-ligand bond, because the distance over which the force acts (i.e., the a value) is much larger in the former case than in the latter case (Bell, 1978). The same reasoning can be applied to delineate the dependence of cell adhesion strength on the bond interaction parameter. As shown in Fig. 10 *B*, a smaller a value causes a rightward shift of the p_d versus f curve. It also broadens the distribution. Fig. 11 *B* illustrates that a serves as a measure of the ease with which the binding energy landscape can be tilted (and hence the energy barrier can be abolished) by the externally applied forces. For the same interaction energies (same K_a^0), an increase in the bond interaction parameter decreases the adhesion strength.

DISCUSSION

Applicability to other cellular and molecular systems

We have also conducted studies to explore the applicability to other cells and molecular systems of the method developed herein. Fig. 12 *A* shows the data of HL-60 cells binding to an E-selectin-coated surface, along with the theoretical curve and evaluated parameters. Good agreement was found between the measured and predicted adhesion fractions. Moreover, the bond interaction parameter a obtained using HL-60 cells is consistent with that obtained using the Colo-205 cells, supporting it as a molecular property independent of the cell type.

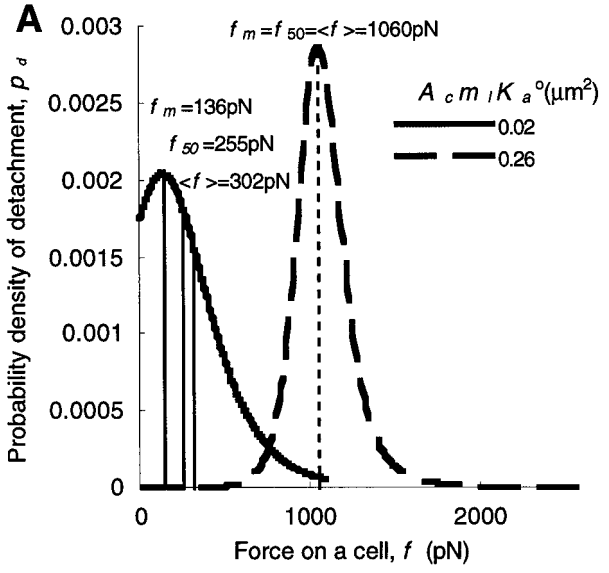

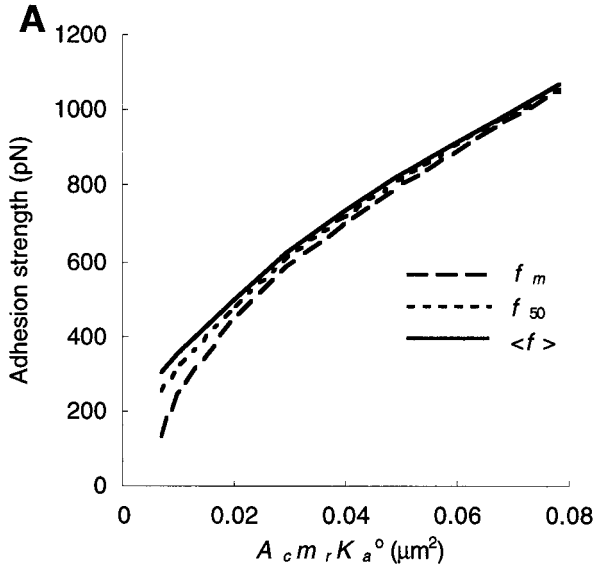

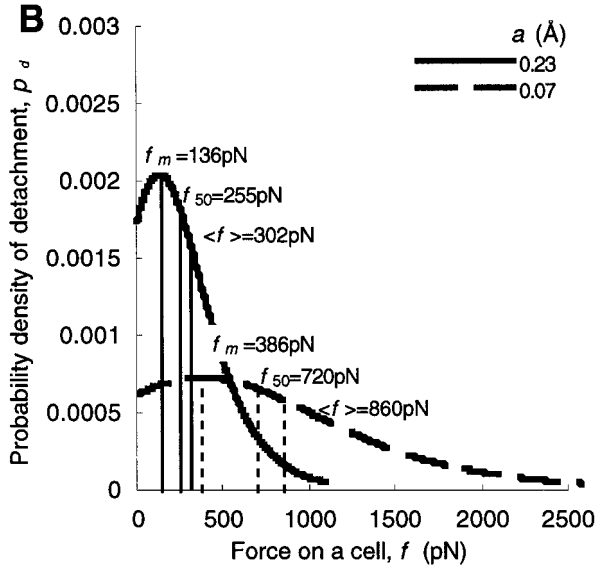

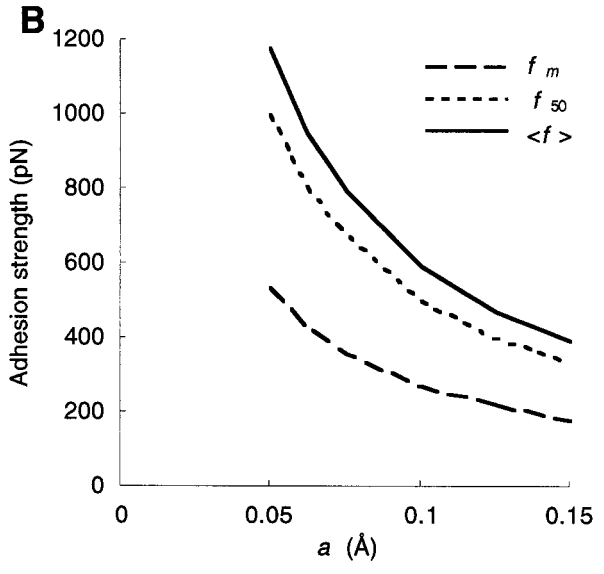

FIGURE 10 Probability density of cell detachment as a function of dislodging force (parameters: $b = 1$, $c = 0$, $m_r = 60$ sites/μm^2). Three statistical definitions of the critical detachment force are shown: most probable force f_m, 50 percentile force f_{50}, and average force $\langle f \rangle$, of cell detachment. (*A*) The density curve shifts right and narrows its shape with an increase in $A_c m_l K_a^0$. (*B*) The density curve is right-shifted and broadened by a decrease in a. Also shown are the corresponding changes in the statistical definitions of adhesion strength.

FIGURE 11 Predicted changes in the three statistical definitions of cell adhesion strength (f_m, f_{50}, and $\langle f \rangle$) with changes in intrinsic parameters, no-load affinity $A_c m_l K_a^0$ (*A*) or bond interaction parameter a (*B*), when all other parameters remain constant ($b = 1$, $c = 0$, $m_r = 60$ sites/μm^2).

Ushiyama et al. (1993) studied adhesion of HL-60 cells to 96-well plate surfaces coated with varying densities of several P-selectin constructs. Instead of centrifugation, these authors inverted the plate to let gravity detach the nonadherent cells. Comparison of their data with our model prediction (Fig. 12 *B*) showed satisfactory agreement and yielded values of $A_c m_l K_a^0 = 0.03$ μm^2 for the truncated and spliced forms and $A_c m_l K_a^0 = 0.08$ μm^2 for the full-length construct. These values are comparable to the values presented in Table 1.

Experiments using freshly isolated human granulocytes, by contrast, were unsuccessful (data not shown). It is believed that adhesion mechanisms other than the E-selectin/carbohydrate ligand pathway dominated the adhesion of a subpopulation of granulocytes in our experimental system. This manifested as significant granulocyte adhesions to 96-well plates coated with or without the E-selectin construct (capture antibody alone or BSA only). Direct microscopic observation confirmed that this adherent fraction corresponded to granulocytes that had spread on the sub-

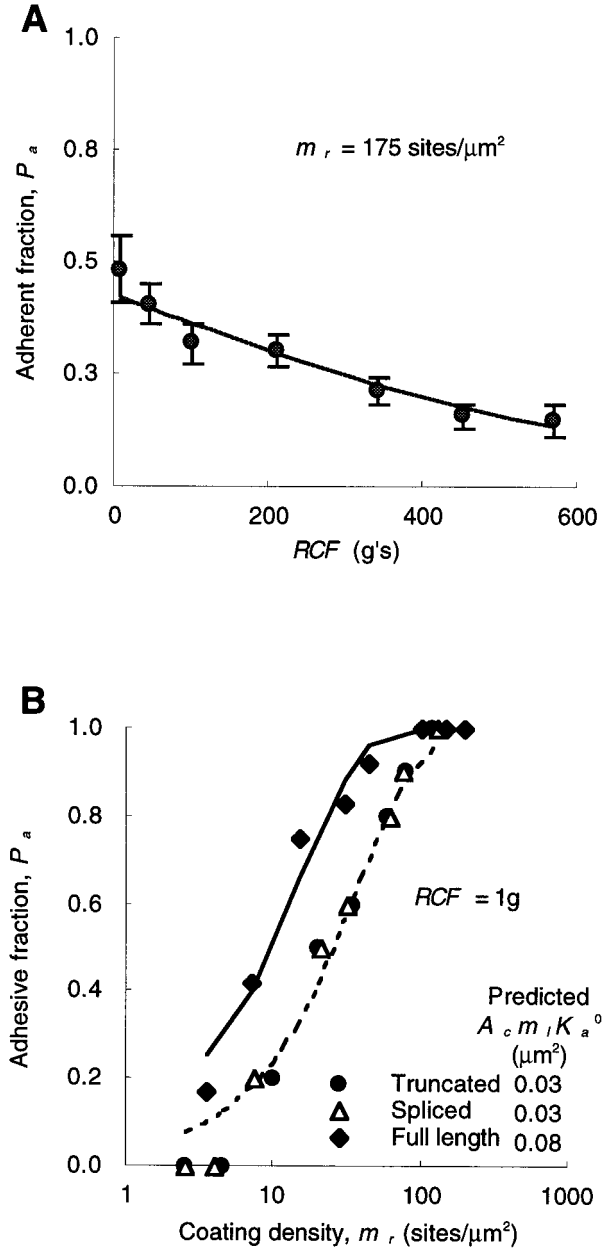

FIGURE 12 (*A*) Adhesion of HL-60 cells to plastic plates coated with ~175 sites/μm^2 E-selectin and subjected to various RCFs. The data (*points*) were compared with the theoretical prediction (*curve*) based on a two-parameter fit (parameters: $A_c m_l K_a^0 = 0.0032$ μm^2 and $a = 0.26$ Å; b was set to be 1). (*B*) Adhesion of HL-60 cells to microtiter well surface coated with P-selectin. The data (*points*; reproduced from Ushiyama et al., 1993, by permission) were compared to prediction (*curves*) to evaluate the value of $A_c m_l K_a^0$ (= 0.03 μm^2 for the truncated and spliced forms, and $A_c m_l K_a^0 = 0.08$ μm^2 for the full-length construct; a was held at a constant value of 0.4 Å; Alon et al., 1997) that best fit the data. Holding the bond interaction parameter constant is justified, for it could not be reliably obtained as the cells were detached by sedimentation under gravity. See text for the limitations of the method under such an extremely low force (1*g*) condition.

strate surface. By comparison, both Colo-205 and HL-60 cells appeared to maintain their round shape on E-selectin for more than an hour. Not only might the adhesion of spread granulocytes be mediated by many more bonds (exceeding the total number of E-selectin molecules in the coated contact area, but its detachment also was likely to occur (if a sufficiently large force were to be applied) as peeling at the edge of the much larger contact area rather than as stretching of all of the bonds. The former was consistent with the much greater adhesion strength of these spreading granulocytes, which could not be detached by even the highest RCF (~ 800*g*) employed in the present study. The latter type of peeling detachment, which has been observed in the micropipette experiments (Zhu et al., 1994), violated the assumptions underlying our model. The above discussion reveals a difference between our experimental system and the one used in McClay's (1981) original work. It also points out limitations of the present method. The method is not applicable to interactions where the cells spread or form excessively strong adhesions with the substrate.

Comparison with binding characteristics derived from other experiments

The flow chamber technique has been used to measure the dependence of the reverse rate coefficient on force (Alon et al., 1995, 1997; Chen et al., 1997). If the forward rate coefficient were constant, then $A_c m_l K_a \propto 1/k_r$. For comparison, the $1/k_r$ versus f data measured via flow chamber experiments (Alon et al., 1997) are also plotted in Fig. 6; they show very good agreement, apart from a proportionality constant, with the $A_c m_l K_a$ versus f data measured via the present centrifugation experiments. The dependence of k_r on f was modeled using the Bell formulation (the $b = 1$ and $c = 0$ case) to predict the value of bond range, a (Alon et al., 1995, 1997). For neutrophils interacting with purified E- or P-selectin reconstituted into a glass-supported lipid bilayer, the value obtained was $a = 0.30$ and 0.40 Å, respectively. Considering the possible differences in the ligand types, the former value compares favorably to 0.26 Å (obtained using HL-60 cells) and 0.20 Å (Table 1, $b = 1$, average of data sets) of this work. The latter value, when combined with the data of Ushiyama et al. (1993) on HL-60 cell adhesion to P-selectin coated plates, produced an affinity ($A_c m_l K_a^0 = 0.03$ μm^2; Fig. 12 *B*) that is comparable to the affinity determined for Colo-205 cell adhesion to E-selectin in the present work. This ability to arrive at similar values by measuring the bond range in two very different experiments (i.e., dynamic versus static assays) supports the nature of this parameter as a physical characteristic intrinsic to the selectin/carbohydrate ligand bonds.

The per-cell forward and reverse (i.e., $A_c m_r m_l k_f$ and k_r) rate constants of human granulocytes interacting with interleukin-1 (IL-1) activated human umbilical endothelial cells (HUVECs) have been estimated, also by using the flow chamber technique, which yielded a value of cellular binding avidity of $A_c m_r m_l K_a = 1.5$ (Kaplanski et al., 1993). (Different notations (k_+ and k_-) were used by Kaplanski et

al. (1993).) Because a very low shear rate was used by these authors to ensure that the forces acting on an E-selectin-carbohydrate ligand bond would be lower than the anticipated single bond strength, the avidity these authors measured should approximate its no-load value. Using an E-selectin density of ~750 sites/μm^2 measured via radioimmunoassays on IL-1-stimulated HUVECs (data not shown), we calculated a value of $A_c m_l K_a = 0.002\ \mu m^2$ for their system. This value is one order of magnitude lower than our measurement of $A_c m_l K_a = 0.02\ \mu m^2$ for the Colo-205 cells (Table 1, $b = 1$). This is probably due to the much smaller contact area that moving granulocytes could make with the stationary HUVEC surface in the flow chamber than that in our static centrifugation assay. Other possible differences between the two experiments that may contribute to the discrepancy in the affinity measurements include the ligand types and their densities.

Dustin et al. (1996) determined the 2D K_a for LFA-3/CD2 interactions and compared it with the corresponding 3D binding affinity for the same receptor/ligand system. These authors reported a 2D K_a of 0.05 μm^2 and a $h \approx 6$ nm for their system. The latter parameter, called the height of the confinement region, was calculated from the ratio of 3D to 2D K_a's (Bell et al., 1984); and its value has been estimated theoretically to be on the order of 10 nm (Lauffenburger and Linderman, 1993). Assuming that $A_c \approx 1\ \mu m^2$ and $m_l \approx 100$ sites/μm^2 (this study, estimated from Fig. 5 *B*) or 63 sites/μm^2 (Ushiyama et al., 1993, calculated from their measurement of 36,000 sites/HL-60 cell), the 2D K_a's estimated using our method (~2×10^{-4} and $5 \times 10^{-4}\ \mu m^2$ for the E- and P-selectin/carbohydrate ligand bonds, respectively) are two orders of magnitude smaller than that measured by Dustin et al. (1996) for the LFA-3/CD2 bonds. Using the published 3D K_a values of 0.5 mM^{-1} (Cooke et al., 1994) to 10 mM^{-1} (Jacob et al., 1995), along with the 2D K_a determined in this work, the height of the confinement region can be estimated to range from 4 to 70 nm for the Colo-205 cell adhesion to an E-selectin-coated surface. By comparison, the h value for the P-selectin/carbohydrate ligand case, calculated using the 3D K_a (~10 μM^{-1}) reported by Ushiyama et al. (1993) and the 2D K_a that we evaluated from their data, is 50 μm, four orders of magnitude higher than the theoretical range.

Roles of molecular diffusion and cell movement

Factors other than the difference in the molecular systems may also contribute to the difference of two orders of magnitude between the 2D K_a values determined by the present work and those by Dustin et al. (1996). One such factor may be lateral mobility of the molecules, as diffusive transport is usually the limiting step in the two-step binding process (the other step being intrinsic reaction) when both molecular species are surface-linked (Lauffenburger and Linderman, 1993). The dominating diffusion coefficient in the experimental system of Dustin et al. (1996) should be the free LFA-3 reconstituted into the lipid bilayer, which was 5.9×10^{-9} cm^2/s. In the centrifugation (or plate inversion) experiments, by contrast, it should be the diffusivity of the carbohydrate ligand on the target cell surface, as the selectins were immobilized on the plastic surface. A typical diffusivity for a cell surface protein is on the order of 10^{-10} cm^2/s (Jacobson et al., 1987). Existing theories have shown that diffusion influences both the forward (k_f) and reverse (k_r) rate constants but not the equilibrium constant (K_a) as its effects cancel each other in the ratio (Lauffenburger and Linderman, 1993). This may apply to the experiment of Dustin et al. (1996), where the cells were allowed to sit on the substrate, as the effect of fast diffusion of the receptors and ligands is bidirectional, i.e., it enhances both their abilities to form the so-called encounter complexes (Bell, 1978) before intrinsic association occurs and to escape the encounter complexes after intrinsic dissociation occurs. However, it may not apply to our centrifugation experiment, where the cell was pulled away from the surface by an external force once the last bond was broken. The added movement of the cell is likely to increase the ability of the ligand to escape the encounter complex, thereby enhancing the (apparent) effect of diffusion on $k_r^{(1)}$. It should be noted that such an effect is unidirectional, i.e., not only may it increase $k_r^{(1)}$, but it may also decrease $k_f^{(1)}$ by acting against the ligand's efforts to form an encounter complex with the receptor, thereby diminishing the possibility of intrinsic binding ($k_f^{(n)}$ and $k_r^{(n)}$, where $n > 1$ should not be affected). If adhesion is mediated by a small number of bonds, then the contribution of $k_f^{(1)}/k_r^{(1)}$ to the overall binding affinity (given by Eq. 8 as a statistical average) would be significant.

To obtain a quantitative estimate for the above effect, the time for a cell under centrifugal force to move away from a wall was calculated based on the creeping flow theory (Happel and Brenner, 1963). The result shows that it would take only 0.5 ms for a smooth sphere 10 μm in diameter, subject to a 800*g* body force, to move from a gap distance of 5 nm (which is an underestimated length for a capture antibody-E-selectin construct-ligand complex linking the cell to the wall) to 105 nm (which is probably an overestimated separation distance for $k_f^{(1)}$ to vanish). For a molecule to move the same distance in the same time by diffusion, an "equivalent diffusivity" of 2×10^{-7} cm^2/s would be required. With such an added unidirectional movement (which is orders of magnitude larger than the molecule's own diffusion), $k_r^{(1)}$ may no longer be transport limited and $k_f^{(1)}$ may be diminished. Therefore, the K_a^0 measured by our method may be much smaller than values measured by another method that does not involve separating the cells, such as the method of Dustin et al. (1996). This line of reasoning is also consistent with measurements by us (Chesla et al., unpublished work) and others (Pierres et al., 1995), which show that, although both have the same dimension (1/s), the reverse rate, k_r, for dissociation from a ligand-coated surface of a receptor bound to cells or beads measured by their detachment is orders of magnitude

greater than that of the very same receptor measured when it dissociates into solution. Moreover, this discussion suggests that caution must be exercised when applying the 2D affinity measured by the present method to a situation where cell detachment is not involved, such as the case of Dustin et al. (1996), or vice verse.

Justifying the probabilistic formulation

The generalization from a deterministic kinetic model to its corresponding probabilistic formulation necessitates solving a system of coupled ordinary differential equations (Eq. 1) instead of just one such equation, which represents a major increase in the mathematical complexity of the problem. Because both the deterministic and probabilistic models provide the same information as the system size becomes large, it is of interest to examine the number of bonds mediating cell adhesion in our centrifugation assay to see if the probabilistic formulation is warranted. Using the fitted parameters ($A_c m_l K_a^0$ and a) from Table 1 (for $b = 1$ and $c = 0$), the subpopulations of cells having various numbers of bonds were calculated with Eq. 3 and plotted in Fig. 13 *A*. It can be seen that, even when the adherent fraction was as high as 73%, the majority of cells were bound by only a few (<5) bonds (to the surface coated with an E-selectin density of 60 sites/μm^2 and subject to no force). Also predicted was how the average number of bonds, $\langle n \rangle$, per adherent cell and its fluctuation (represented by the standard deviation, σ_n) would vary with changes in applied force (Fig. 13 *B*). Again, the average number of bonds was small (<2 bonds/adherent cell), even with no applied separation force. In contrast, the standard deviation was large (comparable to $\langle n \rangle$). Such a surprisingly small bond number and significant fluctuation evidently point to the inadequacy of the deterministic model and argue for the use of the probabilistic model.

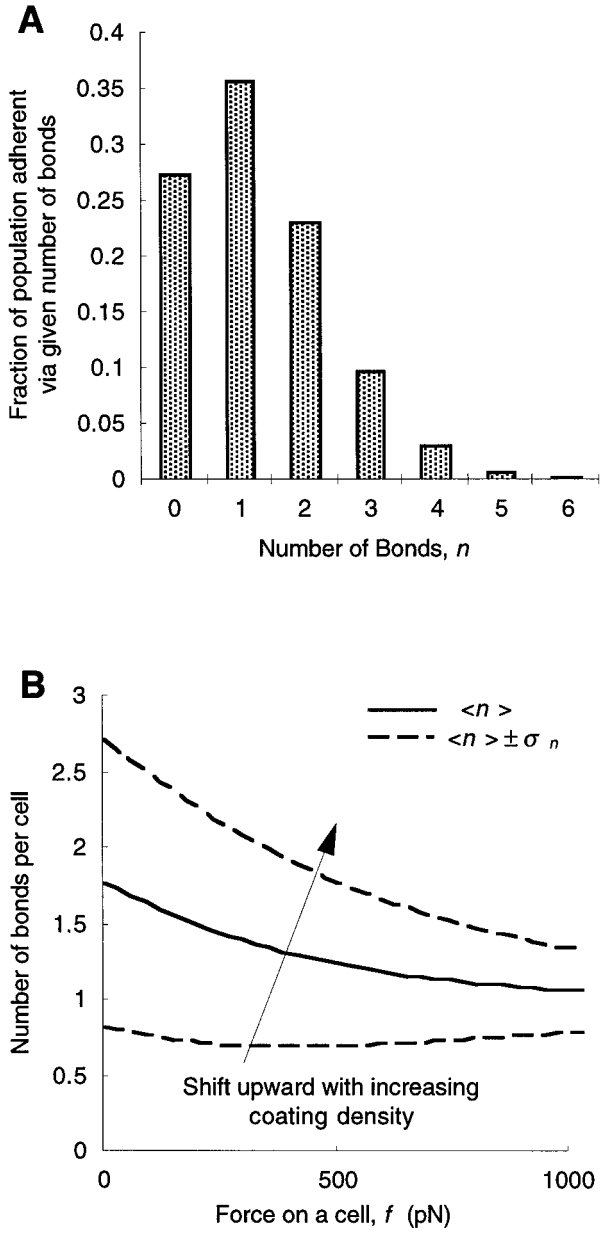

FIGURE 13 (*A*) Predicted probability distribution, p_n, of the number of bonds, n, formed between a Colo-205 cell and the E-selectin-coated surface (parameters: $b = 1$, $c = 0$, $A_c m_l K_a^0 = 0.0218$ μm^2, $a = 0.225$Å, $m_r = 60$ sites/μm^2, and $f = 0$). (*B*) The average number of bonds per adherent cell $\langle n \rangle$ (*solid curve*) $\pm$ SD σ_n (*dashed curves*) as functions of the dislodging force (parameters: same as in *A*, except that f was allowed to vary freely).

Consequences of small bond number prediction

As discussed in previous sections, consequences of the small bond number prediction include that the dependence of the cell adhesion strength on binding affinity may be stronger than logarithmic and that the 2D K_a measurement by the present method may be lowered by the cell movement. Here we discuss another consequence. In addition to the 3D affinity, a by-product that can be simultaneously measured in experiments using the existing methods such as the Scatchard analysis is the total number of carbohydrate ligands on the cell surfaces (Ushiyama et al., 1993). Because m_l also appears in Eq. 3 as a separate parameter, it may seem possible, at least in principle, to determine its value from curve fitting of the predicted to measured P_a versus RCF and m_r relationships. Attempts to do so were unsuccessful (not shown). This was attributed to the number of bonds with nonvanishing probabilities being much smaller than both the numbers of receptors and ligands in the contact area available for binding. Under this condition, Eq. 3 is reduced to Eq. 5. As pointed out previously, in this case the per-molecule density no-load binding affinity can no longer be separated from the ligand density. It was the grouped quantity, $A_c m_l K_a^0$, that was determined from the P_a versus RCF and m_r data. In other words, to dissect the per-molecule density binding affinity requires separate measurements of m_l from independent experiments.

Validity of the small bond number prediction

Because the small bond number prediction appeared counterintuitive and because it has far-reaching implications (above), it was felt warranted to reexamine its validity more carefully. As an alternative, the large bond number limit of model I was considered (model II; see Appendix). The effect of cell heterogeneity in a population was hypothesized to underlie the fractionalization seen in the adhesion data. Model II is falsified in the Appendix by its inability to account for the data with reasonable parameter values and by the substantial discrepancies between its predictions and measurements.

Fig. 14 shows the probability of having single and multiple bonds as a function of the adhesion fraction and centrifugal force derived from Eq. 5. It can be viewed as a precise quantitative expression of the verbal arguments used by several authors to infer the small bond number hypothesis from the low frequency of cell adhesion (e.g., Evans, 1995). Thus, as binding becomes infrequent (<30%), the adhesion is predicted to be dominated by single bond events. When this prediction is applied to an experiment, it has implicitly assumed that the assay is sufficiently sensitive to detect adhesions as weak as those mediated by a single bond, such that the reported low adhesion frequency is not due to a limited ability to detect binding at the low force end. At fixed E-selectin densities, the adhesion fractions increased continuously with decreasing RCF to as low as 8*g* (Fig. 10); and the extrapolation of the curves to 1*g* was in good agreement with those measured in the plate inversion experiment (i.e., detachment via gravity alone; data not shown). At this low end, the corresponding dislodging force acting on a Colo-205 cell was on the order of 0.5 pN, much lower than the force most bonds can sustain.

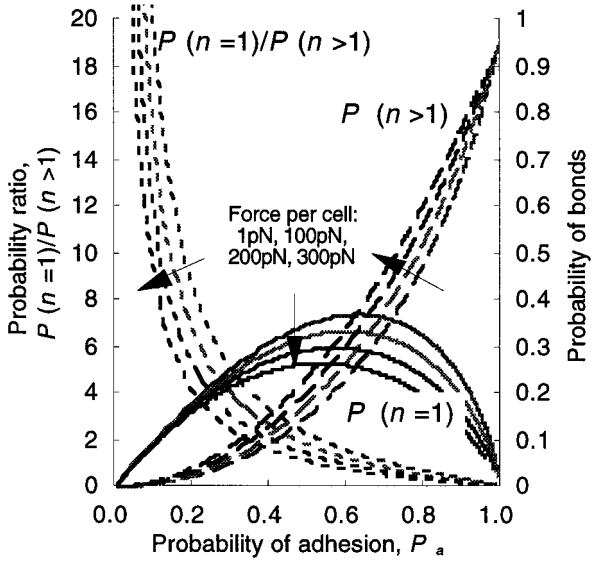

FIGURE 14 The predicted probabilities of a cell adherent via a single bond (*solid curves, right ordinate*) and multiple bonds (*dashed curves, right ordinate*), as well as the ratio between the two (*dotted curves, left ordinate*) as functions of the adhesive fraction and dislodging force (parameters: $b = 1$, $c = 0$, $A_c m_l K_a^o = 0.0218\ \mu m^2$, $a = 0.225$ Å). As the adhesion fraction decreases (say, below 0.3), the single bond binding dominates the adhesion events.

It cannot be emphasized enough that the small bond number prediction is valid if and only if the underlying assumptions for the master equations are valid. A careful inspection of Eq. 1 revealed that it would have predicted exactly the same functional form of a solution equally capable of fitting the data and estimating the same cellular binding avidity and other model parameters, if n in the master equations were to represent, instead of the number of bonds, the number of attachments, each of which, in turn, consisting of a cluster of m bonds. Then m_r and m_l would have to be interpreted as, respectively, the densities of their clusters, instead of the densities of the receptors and ligands themselves. This would have resulted in an m^2-fold increase in the per-molecule binding affinity. This possibility cannot be ruled out by the fact that our data favor the probabilistic (model I) over the deterministic (model II; see Appendix) description for binding kinetics. Furthermore, we wish to emphasize that, in contrast to what has been suggested by others (Capo et al., 1982; Pierres et al., 1995), this possibility cannot be ruled out by the apparent linear dependence of adhesion fraction on the receptor density (cf. Fig. 5 *A* and the text regarding the monovalency of E-selectin binding). The favorable comparison between binding characteristics measured by the present work and those derived from flow chamber experiments, although appealing, should not be counted as valid supporting evidence for the small bond number prediction. The flow chamber experiments also assumed, based on the same probabilistic arguments used here, that their measurements were made on a single bond basis. Therefore, it would be circular to use the agreement between the two experiments to support each other.

In view of the presence of numerous microvilli on the tips of which adhesions presumably occur, clustering of the carbohydrate ligands on the target cell surfaces may be possible. However, there was no reason to believe that the E-selectin immobilized on the plastic surface was not uniformly distributed. It is even more difficult to envision that all of these randomly formed clusters would have exactly the same number of m molecules. Additional evidence against the clustering hypothesis came from the fact that Eqs. 3 and 5 fitted the experimental data equally well (in Fig. 10, the theoretical curves predicted by the two equations are indistinguishable because the differences are smaller than the thickness of the curves) and predicted the same values for the model parameters ($A_c m_l K_a^0$, as well as a, b, c, and d). This was expected if and only if the numbers of both receptors and ligands in the contact area available for binding excessively outnumber that of the attachments that have nonvanishing probabilities, regardless of whether an attachment represents a bond or a clusters of bonds, because it is precisely the condition under which Eq. 5 approximates Eq. 3. Because the E-selectin coating densities were measured on a per-site (not per-cluster) basis, the lack of difference between the predictions derived from Eqs. 3 and 5,

even when the E-selectin coating density was as low as ~ 10 sites/μm^2, suggested that the clusters (if there were clustering) should have consisted of only a small number of bonds. For example, if we take 5 as the number of attachments that have nonvanishing probabilities (cf. Fig. 13) and assume a contact area $A_c = 3\ \mu m^2$ (probably an overestimated value), then for $A_c m_r/m$ ($= 30/m$) to excessively outnumber 5 (e.g., by a factor of 3), m could be no greater than 2. The above considerations, although they cannot rigorously prove it, do favor the small bond number hypothesis.

A paradox associated with the steady-state hypothesis

A key assumption of the present work is the achievement of steady state. Whereas the results from several experiments designed to test this contention appear to be supportive (cf. Figs. 4 and 5), these experimental results, when combined with the small bond number prediction and fast kinetic rate measurement, lead to an apparent paradox. The existence of a steady state implies dynamic equilibrium not only at the molecular level of bond formation and breakage, but also at the cellular level of attachment and detachment. On the molecular level, the short lifetime (1–2 s) of E-selectin/carbohydrate bonds (Kaplanski et al., 1993; Alon et al., 1997) implies that the bonds must be constantly broken and reformed. On the cellular level, dynamic equilibrium seems not to be favored in the centrifugation assay. A detached cell can reattach only if it remains near the E-selectin-coated surface, for it would lose this ability permanently once it has moved sufficiently far away from the surface, because interactions would no longer be possible. Considering the small number of molecular bonds predicted to support cellular adhesions, it may seem that over time more and more cells will become separated from the surface. The fact that this was not observed experimentally (Fig. 4 *A*) is intriguing, and we have not yet found a satisfactory theoretical resolution to this apparent paradox. The explanations below represent the best hypotheses (each with a counter-argument) that we can put forth at this point. If one accepts the small bond number prediction (based on the discussions in the preceding sections), then either of the following must be true: 1) after a cell becomes bond free, the time it took for the cell to move beyond the reach of the receptors was longer than that for new bond formation so the cell could be recaptured; or 2) the time for bond rupture was prolonged by force such that dissociation did not occur in the duration of spinning.

The time scale of bond formation, $(A_c m_r m_l k_f)^{-1}$ ($= 0.5$–3 s, for $m_r = 200$–30 sites/μm^2), can be estimated using the measured binding affinity, $A_c m_l K_a^0$ ($= 0.023\ \mu m^2$, average of Colo-205 data; Table 1, $b = 1$), and the reported reverse rate constant, k_r (≈ 0.5–0.7/s; Kaplanski et al., 1993; Alon et al., 1997), or from our direct measurement (Piper, 1997; see below). Although the calculation in the previous section showed that it might take a much shorter time (~0.5 ms) for a smooth sphere to move away from the wall, this result may not be extrapolatable to the case of a rough sphere, as this calculation depends critically on the gap distance at which the movement starts and ends (Happel and Brenner, 1963). A cell of rough surface may have a Stokes radius slightly larger (say by 0.2%) than the one that is directly measured from the membrane. This would place the Stokes radius closer (say, by 20 nm) to or even at the physical substrate surface at the time when the cell begins to move away from the surface. This could yield a duration required for a cell to move sufficiently far to preclude receptor/ligand interactions that is even longer than the time scale of bond formation. The difficulty of this hypothesis is that it fails to explain why some cells were able to move away from the surface in a very short period of time (~1 min) and, after that, other cells were not able to move away in a much longer period of time (~15 min; Fig. 4 *A*).

We have recently employed the micropipette technique to measure the kinetic rates and the dependence on force thereof, using the identical E-selectin reagents and Colo-205 cells used in this work (Piper, 1997). In the absence of force, the per E-selectin density cellular forward rate constant was found to be $A_c m_l k_f = 0.01\ \mu m^2$/s, and the reverse rate constant $k_r = 0.35$/s, which yielded an $A_c m_l K_a^0 = 0.029\ \mu m^2$, which is in good agreement with the value obtained in the present study. When a force was applied, however, the reverse rate coefficient was found to first increase with force until it achieved a maximum of 1.8/s at 17 pN; thereafter it decreased with force to 0.51/s at 30 pN (the high end of forces examined). The latter type of response, called catch bond behavior, could allow the lifetime of a bond to be prolonged by the applied force, even to a point at which dissociation would become impossible (Dembo et al., 1988; Dembo, 1994). Additional experiments are under way to determine whether the catch bond behavior continues beyond the force range examined in the study of Piper (1997) into that of the present work, i.e., ~100 pN. Should this be the case, then the steady-state paradox could be resolved by the catch bond concept. The difficulty of this hypothesis is that it fails to explain why the detached fraction measured in this work continued to increase with increasing force. In any event, it is our hope that the apparent contradiction among the steady-state observation, fast kinetic rate measurement, and small bond number prediction described herein would stimulate further investigations of bond dissociation under force.

CONCLUSION

This work introduces a novel method of measuring the two-dimensional binding parameters, a and K_a^0, of a receptor/ligand pair mediating adhesion. The method should be easy to implement, as the experiment is a commonly used centrifugation assay and the theory resulted in simple closed-form solutions. The simplicity of the assay afforded

well-controlled experimental conditions and a large amount of high-quality data. This allowed for decisive selections, not only between two proposed mechanisms for adhesion fractionalization, but also among various constitutive equations relating bond dissociation to force. The analytical solution provides important predictions about a variety of physical and chemical parameters relevant to cell adhesion. The model has been supported by 1) careful experimental validation of the underlying assumptions, 2) good agreements between data and predictions, and 3) consistency between parameters estimated by the present method and those reported in the literature. It also has a fundamental difficulty that requires further studies to resolve.

APPENDIX

Model II: effect of heterogeneity of cells on their detachment

In the large system limit (i.e., as $\langle n\rangle \to \infty$), the various definitions of cell adhesion strength given by Eq. 7a–c yield the same value because the distribution given by Eq. 6c approaches a Dirac delta function. This can be seen in Fig. 10 *A*, where a larger $\langle n\rangle$ (as a result of an increase in $A_c m_l K_a^0$) is shown to cause the probability of cell detachment to become less broadly distributed. In other words, at the individual cell level, detachment becomes deterministic, as a defined force emerges below which the cell will stay adherent and above which detachment will occur. To explore this possibility, an alternative model, model II, was investigated (Zhu et al., 1991). In contrast to model I, which emphasizes the intrinsic stochastic nature of bond formation and breakage at the molecular level, but assumes an ensemble of identical cells, model II postulates that the observed fractionalization of adhesion is due to the heterogeneity of cell population, but assumes defined values for single bond strength, f_b, and bond number, $\langle n\rangle$, for a given cell. Thus, for a particular cell subject to a RCF, the deterministic criteria for it to remain adherent are expressed as the requirement that the dislodging force not exceed the sustainable adhesive force, namely,

$$f = \mathrm{RCF} \times V\Delta\rho < \langle n\rangle f_b \tag{A1}$$

where V is the cell volume and $\Delta\rho$ is the difference in mass densities of the cell and the suspending medium. The bond number is given by the deterministic limit of Eq. 8.

Determination of cellular heterogeneity

In Eq. A1, the cell properties that may be variable in a population are mass density and volume. Furthermore, the average bond number, $\langle n\rangle$, depends on the ligand expression on the cell. Cell densities were measured by centrifugation through a continuous density gradient. The density gradient was established by adding 4.9 ml of Percoll to 4.2 ml 2× PBS, and then centrifuging for 40 min at 15,000 rpm in a JA-20 rotor (Becton Dickinson). Samples of Colo-205 or HL-60 cells were then overlaid on the gradient, along with calibration beads (Polyscience, Warrington, PA). The cell-gradient mixture was spun at 1500 rpm for 25 min. Density was determined by comparing the final level of the cell layer to the levels of the calibration beads, which yielded mean values of 1.052 and 1.054 g/cm^3 for the Colo-205 and HL-60 cells, respectively, with very small variances in large populations of cells.

The cell volume, by contrast, was found by direct measurement to be broadly distributed. Immediately after detachment and splitting of the cell culture, video microscopy was used to measure two perpendicular diameters as calibrated by a stage micrometer. The average diameter was used to compute the volume of the cell (assuming spherical shape). The volume data was collected and analyzed to obtain the size histogram as well as the mean and standard deviation for each cell type. The mean ± SD of volume for the Colo-205 and HL-60 cells were, respectively, 2100 ± 600 and 1300 ± 400 μm^3. The cumulative percentage of the volume histogram can be fitted very well by a lognormal distribution with these means and standard deviations (Fig. 15 *A*). Based on flow cytometry data on many other cell surface molecules, a lognormal distribution was also assumed for the ligand density expressed on the target cells (Fig. 15 *B*).

Relating cellular heterogeneity to adhesion fraction

It follows from Eq. A1 that, for a given cell volume, a cell expressing fewer ligands is more likely to be detached than a cell expressing more ligands by the same centrifugal speed, because the latter cell can form more bonds and hence sustain a larger dislodging force. A "critical ligand density" can be defined from Eqs. 8 and A1:

$$m_{lc}(V) = \frac{\mathrm{RCF} \times V\Delta\rho}{A_c f_b}\left[1 + \frac{1}{K_a(f_b)}\left(m_r - \frac{\mathrm{RCF} \times V\Delta\rho}{A_c f_b}\right)^{-1}\right] \tag{A2}$$

For a population of cells with the same volume, model II assumes that the adherent fraction is determined by the percentage of cells in the population whose ligand expression levels are higher than m_{lc}, which can be calculated as the area under the lognormal distribution curve and right of the vertical line $m_l = m_{lc}$ (Fig. 15 *B*):

$$P_{a|V} = 1 - \Phi\left\{\ln^{-1/2}\left(1 + \frac{\sigma_{m_l}^2}{\langle m_l\rangle^2}\right)\ln\left[\frac{m_{lc}(V)}{\langle m_l\rangle}\sqrt{1 + \frac{\sigma_{m_l}^2}{\langle m_l\rangle^2}}\right]\right\} \tag{A3}$$

where $\Phi(\cdot)$ denotes the cumulative normal distribution function. $\langle m_l\rangle$ and σ_{m_l} are, respectively, the mean and standard deviation of the ligand expression level.

Taking $P_{a|V}$ as the probability conditioned by the target cell with a volume of V, the total probability, or unconditioned adherent fraction, can be determined by

$$P_a = \frac{\ln^{-1/2}\left(1 + \dfrac{\sigma_V^2}{\langle V\rangle^2}\right)}{\sqrt{2\pi}} \int_0^\infty \exp\left\{-\left[\frac{1}{\sqrt{2}}\ln^{-1/2}\left(1 + \frac{\sigma_V^2}{\langle V\rangle^2}\right)\ln\left(\frac{V}{\langle V\rangle}\sqrt{1 + \frac{\sigma_V^2}{\langle V\rangle^2}}\right)\right]^2\right\}\frac{P_{a|V}}{V}\,dV \tag{A4}$$

where $\langle V\rangle$ and σ_V are, respectively, the mean and standard deviation of the lognormally distributed cell volume, which has been assumed to be independent of the ligand distribution. A graphic interpretation of Eq. A4 is shown in Fig. 15 *C*.

It should be noted that the effects of heterogeneity in a cell population can be included in the probabilistic model the same way as they were treated in the deterministic limit. Thus Eqs. 3–5 can be viewed as conditioned probabilities for particular values of m_l and V, and the unconditioned probability can be obtained by the total probability formula as in Eq. A4. Here we separate the stochastic effects due to molecular and cellular properties merely for the sake of simplicity. This also allows us to test one aspect at a time, to determine which is more likely to be responsible for the observed adhesion fractionalization.

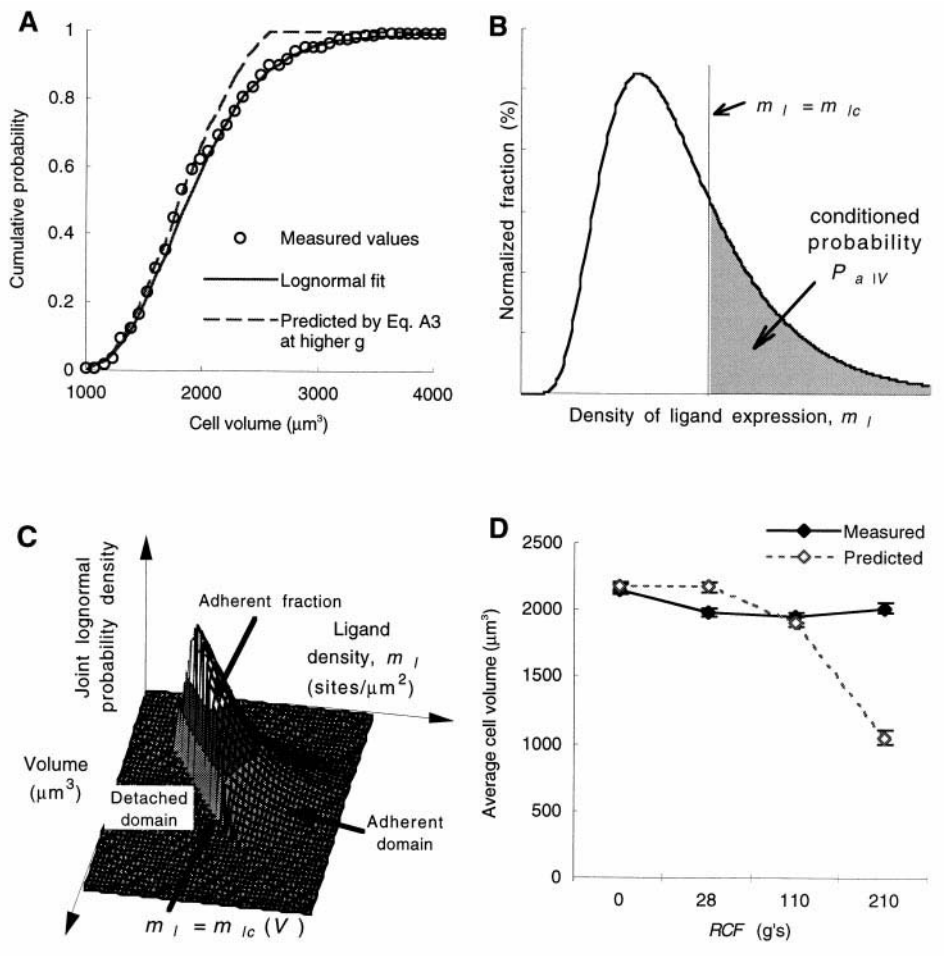

FIGURE 15 (*A*) Indifference of cell volume distribution to centrifugation. The volumes of 575 freshly trypsinized cells were measured microscopically. The measured cumulative percentage (*points*) are best described by a lognormal distribution (*solid curve*) with an average of 2100 μm^3 and a standard deviation of 600 μm^3. The dashed curve represents how the cumulative percentage (i.e., $P_{a|V}$) would have shifted should larger cells be preferentially detached by the centrifugation force as predicted by Eq. A3. The volumes of adherent cells postcentrifugation were also measured, which showed the same distribution as the original population (the data points overlapped, not shown). (*B*) Assumed lognormal distribution for ligand expression in a target cell population. Assuming identical cell volume in the population, the (conditioned) adherent fraction $P_{a|V}$ is shown as the shaded area under the distribution curve and left of the vertical line that defines the critical ligand density, $m_l = m_{lc}$. (*C*) Joint lognormal probability density is plotted as a function of m_l and V over the adherent domain, which is separated from the detached domain by the condition of critical ligand expression, Eq. A2. The (unconditioned) adherent fraction P_a can be calculated as the volume under the surface of the joint lognormal distribution over the adherent domain. P_a increases with increasing m_r and/or decreasing RCF, as the curve separating the two domains shifts, resulting in larger areas of the adherent domain. (*D*) The measured (*solid curve*) and predicted (*dashed curve*, using Model II) mean and standard error of volumes of Colo-205 cells that remained adherent after being subjected to centrifugation at various speeds plotted against the RCF.

Identification of the stochastic aspects responsible for adhesion fractionalization

To identify the stochastic events that underlie the fractionalization of adhesion in a cell population, models I and II were tested for their ability to represent the centrifugation assay by systematically comparing the theoretically predicted with the experimentally measured specific adherent fractions, P_a, over a wide range of m_r and RCF. The lack of saturation at E-selectin densities below 60 sites/μm^2 (Fig. 5 *A*) suggests that the carbohydrate ligands expressed on the Colo-205 cells excessively outnumber the E-selectin coated on the surface. This provides the justification for using the approximation given by the far right-hand side of Eq. 8. Under this condition, Eqs. A2–A4 predict that the two experimentally independent variables, m_r and RCF, can be combined into a single similarity variable, m_r/RCF, such that the family of P_a versus m_r and RCF curves can be collapsed into a single curve when the abscissa (m_r axis) is scaled by RCF. Such a scaling law is predicted to break down when m_r is comparable to m_l, as signified by saturation. Comparison of this prediction with experimental data is shown in Fig. 16. As can be seen, the data deviate from the scaling law more significantly for unsaturating (Fig. 16 *A*) than for saturating (Fig. 16 *B*) E-selectin densities, which contradicts the prediction of model II.

Also tested in Fig. 16 was the ability of the two models to account for the data. For the saturated case, model II was unable to fit the data with a realistic spread of the ligand expression of a cell population, e.g., $\sigma_{ml}/\langle m_l \rangle = 0.5$ (Fig. 16 *B*, *solid curve*), although a fit could be produced by using an unrealistic $\sigma_{ml}/\langle m_l \rangle = 2$ (Fig. 16 *B*, *dashed curve*). Despite the fact that the ligand distribution of the target cells was not measured in this study, other reports do not support the conclusion that such a wide distribution of ligands exists within a cell population (Munro et al., 1992; Norgard et al., 1993; Ohmori et al., 1993; Kunzendorf et al., 1994). For the unsaturated case (Fig. 16 *A*), it is evident that model II was unable to fit the data for either $\sigma_{ml}/\langle m_l \rangle$ value, especially at the low end of the force range.

In contrast, the agreement between measurements and predictions of model I was much more satisfactory (Fig. 16, *C* and *D*), especially for the

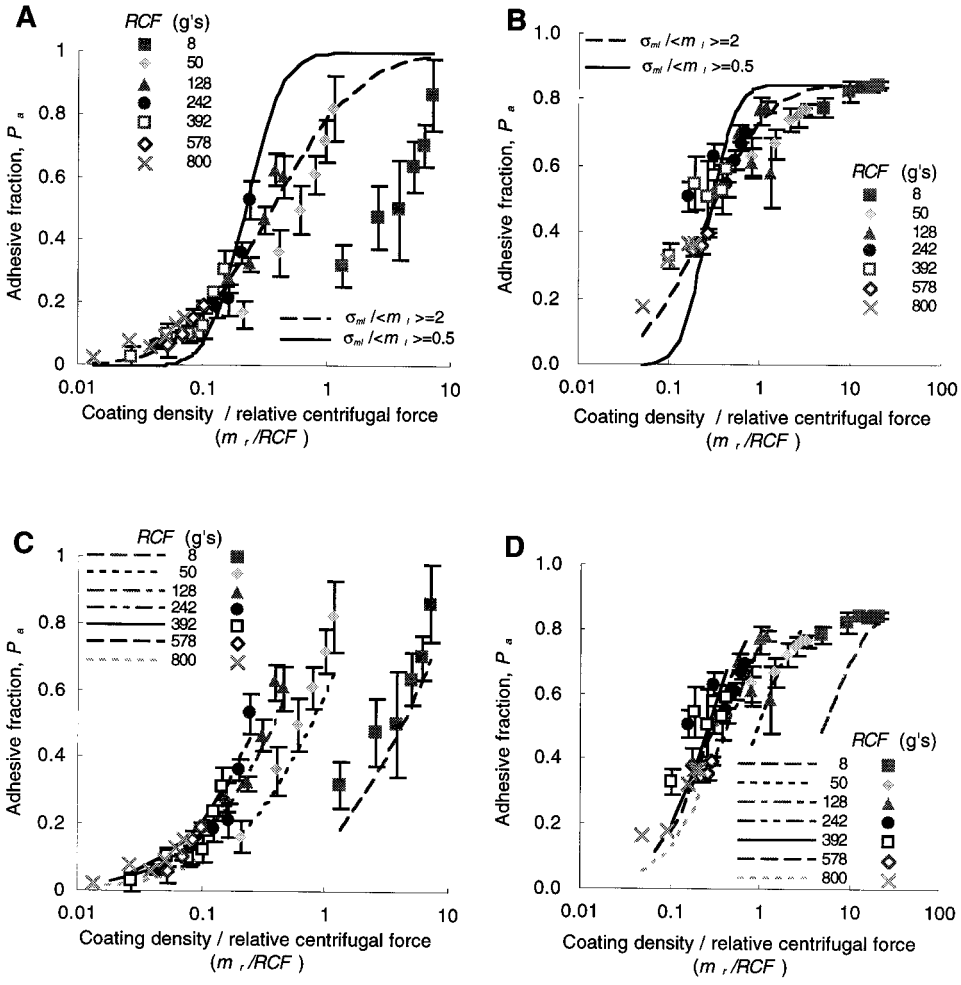

FIGURE 16 Comparison of the abilities of the two models to account for the data. The same experimental data (*points*) as those in Figs. 9 (unsaturated) and 5 *B* (saturated) were replotted as adhesion versus m_r/RCF. Also shown are the predictions (*curves*) of Model II (*A* and *B*) and Model I (*C* and *D*) for the unsaturated (*A* and *C*) and saturated (*B* and *D*) bindings. To test Model II, the same data were fitted using a realistic value ($\sigma_{ml}/\langle m_l \rangle = 0.5$, *solid curves*) as well as a best fitted but unrealistic value ($\sigma_{ml}/\langle m_l \rangle = 2$, *dashed curves*) for the relative variation of ligand expression (best fitting parameters for the dashed curves $A_c\langle m_l \rangle K_a(f_b) = 0.0128\ \mu m^2$ and $f_b = 1.2 \times 10^{-7}$ pN in *A* and $A_c\langle m_l \rangle K_a(f_b) = 0.0187\ \mu m^2$ and $f_b = 1.2 \times 10^{-7}$ pN in *B*). Note that the single bond strength predicted in neither case is reasonable, indicating the inappropriateness of this model. To test Model I, the exponential law ($b = 1$, $c = 0$) was employed to fit the data (best fitting parameters $A_c m_l K_a^o = 0.0218\ \mu m^2$ and $a = 0.225$Å in *C*, and $A_c m_l K_a^0 = 0.0226\ \mu m^2$ and $a = 0.211$Å in *D*). It is evident from direct inspection of *C* and *D* that Model I was able to represent the data for both adhesion sets.

unsaturating data (Fig. 16 *C*) and at larger forces. Model I showed better performance, even when just a simple exponential law ($b = 1$, $c = 0$) was employed, which left us with only two adjustable parameters ($A_c m_l K_a^0$ and a) in the curve fitting. And even better performance was obtained using the power law ($b = 0$, $c = 1$). By comparison, model II had three free parameters ($A_c\langle m_l \rangle K_a(f_b)$, f_b, and $\sigma_{ml}/\langle m_l \rangle$). The contrast between the ability of model I and the inability of model II to describe the experimental data suggests that, although cellular heterogeneity may have some effect, the molecular randomness is more important, as the exclusion of the latter, not the former, significantly reduces the model's ability to account for the data.

Further falsification of model II was obtained from the measurements of volumes of adherent and detached cells after subjecting them to various centrifugal forces. Equation A3 can be viewed as the cumulative distribution of the cell volume, which, by virtue of Eq. A2, is dependent on the relative centrifugal force. Thus model II predicts that, after centrifugation, the remaining adherent cells would have a smaller volume because larger cells are subject to a larger force and hence would be more likely to be detached. This prediction was not supported by the experiment, as the measured volumes of the cells that remained adherent after centrifugation showed the same distribution (Fig. 15 *A*) and mean (Fig. 15 *D*) as the original population before centrifugation. These data justify neglecting cell heterogeneity in model I.

We thank Drs. K. S. Huang, B. Wolitzky, and D. Burns of Hoffmann LaRoche for their generous donation of the E-selectin construct and 1D6 capture antibody.

This work was supported by National Institutes of Health training grant GM08433, National Institutes of Health grant R29AI38282, National Science Foundation grant BCS9350370, and a grant from the Whitaker Foundation.

REFERENCES

Alon, R., S. Chen, K. D. Puri, E. B. Finger, and T. A. Springer. 1997. The kinetics of L-selectin tethers and the mechanics of selectin-mediated rolling. *J. Cell Biol.* 138:1169–1180.

Alon, R., D. A. Hammer, and T. A. Springer. 1995. Lifetime of the P-selectin-carbohydrate bond and its response to tensile force in hydrodynamic flow. *Nature.* 374:539–542.

Bell, G. I. 1978. Models for the specific adhesion of cells to cells. *Science.* 200:618–627.

Bell, G. I. 1981. Estimate of the sticking probability for cells in uniform shear flow with adhesion caused by specific bonds. *Cell Biophys.* 3:289–304.

Bell, G. I., M. Dembo, and P. Bongrand. 1984. Cell adhesion: competition between nonspecific repulsion and specific bonding. *Biophys. J.* 45: 1051–1064.

Bevilacqua, M. P., J. S. Pober, D. L. Mendrick, R. S. Cotran, and M. A. Gimbrone, Jr. 1987. Identification of an inducible endothelial-leukocyte adhesion molecule. *Proc. Natl. Acad. Sci. USA.* 84:9238–9242.

Bevington, P. R., and D. K. Robinson. 1992. Data Reduction and Error Analysis for the Physical Sciences. McGraw-Hill, New York.

Bongrand, P., C. Capo, and R. Depieds. 1982. Physics of cell adhesion. *Prog. Surf. Sci.* 12:217–286.

Butcher, E. C. 1991. Leukocyte-endothelial cell recognition: three (or more) steps to specificity and diversity. *Cell.* 67:1033–1036.

Capo, C., F. Garrouste, A. M. Benoliel, P. Bongrand, A. Ryter, and G. I. Bell. 1982. Concanavalin A-mediated thymocyte agglutination: a model for a quantitative study of cell adhesion. *J. Cell Sci.* 56:21–48.

Chen, S., R. Alon, R. C. Fuhlbrigge, and T. A. Springer. 1997. Rolling and transient tethering of leukocytes on antibodies reveal specializations of selectins. *Proc. Natl. Acad. Sci. USA.* 94:3172–3177.

Chu, L., L. A. Tempelman, C. Miller, and D. A. Hammer. 1994. Centrifugation assay of IgE-mediated cell adhesion to antigen-coated gels. *AIChE J.* 40:692–703.

Cooke, R. M., R. S. Hale, S. G. Lister, G. Shah, and M. P. Weir. 1994. The conformation of the sialyl Lewis x ligand changes upon binding to E-selectin. *Biochemistry.* 33:10591–10596.

Cozens-Roberts, C., D. A. Lauffenburger, and J. A. Quinn. 1990. Receptor-mediated cell attachment and detachment kinetics: probabilistic model and analysis. *Biophys. J.* 58:841–856.

Daneker, G. W., S. A. Lund, S. W. Caughman, C. A. Stanley, and W. C. Wood. 1996. Anti-metastatic prostacyclins inhibit the adhesion of colon carcinoma to endothelial cells by blocking E-selectin expression. *Clin. Exp. Metastasis.* 14:230–238.

Dembo, M. 1994. On peeling an adherent cell from a surface. *In* Lectures on Mathematics in the Life Sciences: Some Mathematical Problems in Biology, Vol. 24. American Mathematical Society, Providence, RI. 51–77.

Dembo, M., D. C. Tourney, K. Saxman, and D. Hammer. 1988. The reaction-limited kinetics of membrane-to-surface adhesion and detachment. *Proc. R. Soc. Lond.* 234:55–83.

Dustin, M. L., L. M. Ferguson, P.-Y. Chan, T. A. Springer, and D. E. Golan. 1996. Visualization of CD2 interaction with LFA-3 and determination of the two-dimensional dissociation constant for adhesion receptors in a contact area. *J. Cell Biol.* 132:465–474.

Erbe, D. V., B. A. Wolitzky, L. G. Presta, C. R. Norton, R. J. Ramos, D. K. Burns, J. M. Rumberger, B. N. Rao, C. Foxall, B. K. Brandley, and L. A. Lasky. 1992. Identification of an E-selectin region critical for carbohydrate recognition and cell adhesion. *J. Cell. Biol.* 119:215–27.

Evans, E. A. 1995. Physical actions in biological adhesion. *In* Structure and Dynamics of Membranes: Handbook of Physics of Biological Systems, Vol 1. R. Lipowsky and E. Sackmann, editors. Elisevier Science BV, Amsterdam. 723–754.

Evans, E., D. Berk, and A. Leung. 1991. Detachment of agglutinin-bonded red cells. I. Forces to rupture molecular-point attachments. *Biophys. J.* 59:838–848.

Evans, E. A., and K. Ritchie. 1997. Dynamic strength of molecular adhesion bonds. *Biophys. J.* 72:1541–1555.

Hammer, D. A., and D. A. Lauffenburger. 1987. A dynamical model for receptor-mediated cell adhesion to surfaces. *Biophys. J.* 52:475–487.

Happel, J., and H. Brenner. 1963. Low Reynolds number hydrodynamics. Martinus Nijhoff, Boston.

Hulme, E. C., and N. J. M. Birdsall. 1992. Strategy and tactics in receptor-binding studies. *In* Receptor-Ligand Interactions: A Practical Approach. E. C. Hulme, editor. Oxford University Press, New York. 63–176.

Jacob, G. S., C. Kirmaier, S. Z. Abbas, S. C. Howard, C. N. Steininger, J. K. Welply, and P. Scudder. 1995. Binding of sialyl Lewis x to E-selectin as measured by fluorescence polarization. *Biochemistry.* 34: 1210–1217.

Jacobson, K., A. Ishihara, and R. Inman. 1987. Lateral diffusion of proteins in membranes. *Annu. Rev. Physiol*. 49:163–175.

Kaplanski, G., C. Farnarier, O. Tissot, A. Pierres, A.-M. Benoliel, M.-C. Alessi, S. Kaplanski, and P. Bongrand. 1993. Granulocyte-endothelium initial adhesion: analysis of transient binding events mediated by E-selectin in a laminar shear flow. *Biophys. J.* 64:1922–1933.

Kramers, H. A. 1940. Brownian motion in a field of force and the diffusion model of chemical reactions. *Physica (Utrecht).* 7:284–304.

Kunzendorf, U., S. Kruger-Krasagakes, M. Notter, H. Hock, G. Walz, and T. Diamantstein. 1994. A sialyl-Le^x-negative melanoma cell line binds to E-selectin but not to P-selectin. *Cancer Res.* 54:1109–1112.

Kuo, S. C., and D. A. Lauffenburger. 1993. Relationship between receptor/ligand binding affinity and adhesion strength. *Biophys. J.* 65:2191–2200.

Lasky, L. A. 1992. Selectins: interpreters of cell-specific carbohydrate information during inflammation. *Science.* 258:964–969.

Lauffenburger, D. A., and J. J. Linderman. 1993. Receptors: Models for Binding, Trafficking, and Signaling. Oxford University Press, New York.

Li, S. H., D. K. Burns, J. M. Rumberger, D. H. Presky, V. L. Wilkinson, M. Anostario Jr., B. A. Wolitzky, C. R. Norton, P. C. Familletti, K. J. Kim, A. L. Goldstein, D. C. Cox, and K.-S. Huang. 1994. Consensus repeat domains of E-selectin enhance ligand binding. *J. Biol. Chem.* 269:4431–4437.

McClay, D. R., G. M. Wessel, and R. B. Marchase. 1981. Intercellular recognition: quantitation of initial binding events. *Proc. Natl. Acad. Sci. USA.* 78:4975–4979.

McQuarrie, D. A. 1963. Kinetics of small systems. I. *J. Chem. Phys.* 38:433–436.

Munro, J. M., S. K. Lo, C. Corless, M. J. Robertson, N. C. Lee, R. L. Barnhill, D. S. Weinberg, and M. P. Bevilacqua. 1992. Expression of sialyl-Lewis X, an E-selectin ligand, in inflammation, immune processes, and lymphoid tissues. *Am. J. Pathol.* 141:1397–1408.

Norgard, K. E., K. L. Moore, S. Diaz, N. L. Stults, S. Ushiyama, R. P. McEver, R. D. Cummings, and A. Varki. 1993. Characterization of a specific ligand for P-selectin on myeloid cells. *J. Biol. Chem.* 268: 12764–12774.

Ohmori, K., A. Takada, I. Ohwaki, N. Takahashi, Y. Furukawa, M. Maeda, M. Kiso, A. Hasegawa, M. Kannagi, and R. Kannagi. 1993. Distinct type of sialyl Lewis X antigen defined by a novel monoclonal antibody is selectively expressed on helper memory T cells. *Blood.* 82:2797–2805.

Pierres, A., A.-M. Benoliel, and P. Bongrand. 1995. Measuring the lifetime of bonds made between surface-linked molecules. *J. Biol. Chem.* 270: 26586–26592.

Piper, J. W. 1997. Force dependence of cell bound E-selectin/carbohydrate ligand binding characteristics. Ph.D. thesis. Woodruff School of Mechanical Engineering, Georgia Institute of Technology, Atlanta, GA.

Press, W. H., B. P. Flannery, S. A. Teukolsky, and W. T. Vetterling. 1989. Numerical Recipes in FORTRAN: The Art of Scientific Computing. Cambridge University Press, Cambridge.

Puri, K. D., E. B. Finger, and T. A. Springer. 1997. The faster kinetics of L-selectin than of E-selectin and P-selectin rolling at comparable binding strength. *J. Immunol.* 158:405–413.

Rice, G. E., and M. P. Bevilacqua. 1989. An inducible endothelial cell surface glycoprotein mediates melanoma adhesion. *Science.* 246: 1303–1306.

Sawada, R., J. B. Lowe, and M. Fukuda. 1993. E-selectin-dependent adhesion efficiency of colonic carcinoma cells is increased by genetic manipulation of their cell surface lysosomal membrane glycoprotein-1 expression levels. *J. Biol. Chem.* 268:12675–12681.

Springer, T. A. 1995. Traffic signals on endothelium for lymphocyte recirculation and leukocyte emigration. *Annu. Rev. Physiol.* 57: 827–872.

Takada, A., K. Ohmori, T. Yoneda, K. Tsuyuoka, A. Hasegawa, M. Kiso, and R. Kannagi. 1993. Contribution of carbohydrate antigens sialyl Lewis A and sialyl Lewis X to adhesion of human cancer cells to vascular endothelium. *Cancer Res.* 53:354–61.

Ushiyama, S., T. M. Laune, K. L. Moore, H. P. Erickson, and R. P. McEver. 1993. Structural and functional characterization of monomeric soluble P-selectin and comparison with membrane P-selectin. *J. Biol. Chem.* 268:15229–15237.

Zhu, C. 1991. A thermodynamic and biomechanical theory of cell adhesion: general formulism. *J. Theor. Biol.* 150:27–50.

Zhu, C., J. W. Piper, K. H. Lee, and R. A. Swerlick. 1991. A model of cell detachment by centrifugal force. *In* Advances in Bioengineering: Proceedings of the ASME Winter Annual Meeting, Vol. 20. ASME, New York. 77–80.

Zhu, C., T. E. Williams, J. Delobel, D. Xia, and M. K. Offerman. 1994. A cell-cell adhesion model for the analysis of micropipet experiments. *In* Cell Mechanics and Cellular Engineering. V. C. Mow, F. Guilak, R. Tran-Son-Tay, and R. Hochmuth, editors. Springer-Verlag, New York. 160–181.